UNIVERSITY OF CALIFORNIA, SAN DIEGO

Characterization of PHLPP1 in Adult Mouse Ventricular Myocytes

A thesis submitted in partial satisfaction of the

requirements for the degree Master of Science

in

Biology

by

Katherine Huang

Committee in charge:

Joan Heller Brown, Chair
Michael David, Co-Chair
Richard A. Firtel
Nicole H. Purcell
Nicholas Spitzer

2009

The Thesis of Katherine Huang is approved and it is acceptable in quality and form for publication on microfilm and electronically:

Co-Chair

Chair

University of California, San Diego

2009

DEDICATION

This thesis is dedicated to my parents and grandparents for their unconditional love and support, and to everyone who believes in me. Thank you.

TABLE OF CONTENTS

LIST OF TABLES

Buffers and Media

LIST OF SCHEMES

LIST OF FIGURES

ACKNOWLEDGEMENTS

I would like to acknowledge Professor Joan Heller Brown for her support as the chair of my committee, and my mentor Dr. Nicole Purcell whose guidance and involvement has been immeasurable. I was extremely fortunate to be given this opportunity to further my education under Dr. Brown and could not have asked for a better, more passionate mentor than Nicole Purcell.

I would like to thank each member of my thesis committee for the time, advice, support, and encouragement. Each professor was extremely busy yet still set aside time to meet and discuss my research with me, for that I am so grateful. Thank you Dr. Michael David, Dr. Richard Firtel, and Dr. Nicholas Spitzer for your guidance and time.

Finally, I would also like to acknowledge all the members of the Brown lab, whom without would have drastically detracted from the lab environment and my experience as a graduate student. In particular I would like to thank Dr. Shigeki Miyamoto and Shikha Mishra for always watching out for me and for all the advice and insights. Also, I must thank Dr. F Michael Grimm, for although he is not my thesis mentor, he was my first mentor and taught me a lot. And of course, I cannot forget to thank Mr. Jeffrey Smith for making the lab run so smoothly. I truly enjoyed my time at the Brown lab and the biggest factor was the people.

ABSTRACT OF THE THESIS

Characterization of PHLPP1 in Adult Mouse Ventricular Myocytes

by

Katherine Huang

Master of Science in Biology

University of California, San Diego, 2009

Professor Joan Heller Brown, Chair
Professor Michael David, Co-Chair

The fastest growing cardiovascular disease subclass is heart failure, brought about by factors such as cardiac hypertrophy. The serine/threonine kinase Akt is involved in many cellular processes including cell growth, metabolism, protein synthesis, angiogenesis, and studies have implicated Akt in regulating cardiac hypertrophy depending on Akt intensity, duration, and localization. Growth factors, hormones, and cytokines activate Akt by phosphorylating its activation loop (Thr308) and hydrophobic motif (Ser473). Though extensive research focuses on Akt activation by upstream kinases, the mechanism of inactivation by phosphatases are poorly understood. Our

project focuses on the role of the newly discovered Akt phosphatase PHLPP (PH domain leucine-rich repeat protein phosphatase) in adult mouse ventricular myocytes (AMVM). We hypothesized that removal of PHLPP1 will result in increased Akt phosphorylation at Ser473 after agonist stimulation in AMVM. We generated viable *PHLPP1*$^{-/-}$ mice to investigate physiological activation of Akt. PHLPP1 null AMVM had no overt phenotype differences at baseline compared to wild-type (WT) cells. Myocytes stimulated with the cytokine LIF displayed increased Akt Ser473 phosphorylation with no change at Thr308. Increased phosphorylation at Ser473 corresponded with increased activity as demonstrated by kinase assay, but there was no apparent changes in downstream GSK3 or MDM2 phosphorylation. Lastly, we found earlier Akt phosphorylation at Ser473 in PHLPP1 KO myocytes in cytosolic and nuclear fractions. Our data suggests PHLPP is an important regulator of Akt signaling in AMVM and ultimately the heart where it may be an important regulator of cardiac hypertrophy.

Introduction

Hypertrophy Background and Significance

Diseases affecting the heart and its function remain high in all developed nations of the world. The Center for Disease Control and Prevention (CDC) reports that in the United States, heart disease is the leading cause of death for both men and women [1]. A multitude of conditions is encompassed under cardiovascular disease (CVD), with congestive heart failure (CHF) representing the fastest growing subclass of CVD [2]. Approximately 5 million Americans suffer from CHF with almost 400,000 new cases reported each year at a cost of approximately $12 billion [3]. Despite medical treatment and improvements in the ability to diagnose heart disease, CHF remains a highly lethal condition with an overall survival rate at 5 years of only 30%. In response to diverse stress stimuli, the adult heart undergoes cardiac hypertrophy to increase or maintain cardiac work. Hypertrophy is the growth of individual cardiomyocytes, the contractile cells of the heart, in length and/or width as a means of increasing pump function and decreasing ventricular wall tension [2-4]. Initially hypertrophy is compensatory; although it does not necessarily equate to a disturbance in cardiac function, prolonged cardiac hypertrophy increases the risk of developing heart failure, a condition in which the heart cannot pump enough blood throughout the body [2, 4].

Much research has focused on distinguishing the signaling molecules and molecular pathways involved in the regulation of, or perhaps transition from, adaptive (physiological) to maladaptive (pathological) cardiac hypertrophy. “Physiological” hypertrophy is associated with normal postnatal development, exercise, and pregnancy, because cardiac hypertrophy, as aforementioned, is a compensatory response to increased

cardiac output demand. Physiological hypertrophy is characterized by increased cell diameter in cardiac muscle, increased vascularization, enhanced cardiac function, normal sarcomere organization, and normal pattern of cardiac gene expression without interstitial fibrosis or increased cell death [5, 6]. However, "pathological" hypertrophy is associated with many disease conditions such as hypertension, myocardial infarction, and ischemia in which the stress stimuli applied to the heart is constant, resulting in re-expression of fetal-type genes (i.e. β-myosin heavy chain, β-type natriuretic peptide, atrial natriuretic factor), histological alterations (increased fibrosis), contractile dysfunction (ventricular dilatation), and the transition from an oxidative toward a more glycolytic metabolism (as in the fetal stage)[6-8]. Initial stimuli for cardiac hypertrophy range from biomechanical and stretch sensitive-mechanisms via autocrine or paracrine growth factors like angiotensin II to neurohumoral mechanisms associated with the release of hormones (i.e. thyroid hormone, testosterone), cytokines (i.e. leukemia inhibitor factor (LIF), interleukin-1β, cardiotrophin-1), and peptide growth factors (i.e. endothelin-1, transforming growth factor beta)[2, 9-11]. The regulatory factors activating the heart's molecular response to increased wall stress and the development of hypertrophy also activates membrane bound G-protein coupled receptors, which in turn activates an array of intermediate signal transduction pathways such as Akt, mitogen-activated protein kinases (MAPK), protein kinase C (PKC), and calcineurin-NFAT [4]. Of these signaling pathways, Akt is involved in many cellular processes (i.e. cell growth, angiogenesis, anti-apoptosis) that may be considered desirable in relation to cardiac hypertrophy, but the exact role of Akt in cardiac hypertrophy is controversial.

Importance of Akt Signaling

Understanding the fundamentals of signal transduction that regulate cellular processes is an essential part of comprehending various disease progressions. One such pathway is the IGF1-PI3K-Akt pathway, in which the signaling molecule Akt (also known as protein kinase B) is involved in cell growth, angiogenesis, metabolism, proliferation and apoptosis [12]. The 57-kDa protein consists of a N-terminal pleckstrin homology (PH) domain, a catalytic (kinase) domain and a C-terminal regulatory part containing a hydrophobic motif (HM), and exists as three distinct isoforms: Akt 1, Akt 2, and Akt 3 [12-17]. While each isoform is highly conserved in structure and upstream regulation, Akt 1 is involved in cell growth and expressed ubiquitously, Akt 2 regulates metabolism and is found mainly in insulin-responsive tissues such as the liver, muscle, and kidney, and Akt 3, which is highly expressed in the brain, is required for normal brain size and cell number [5, 15, 18, 19]. Akt 1 and Akt 2 are the predominant isoforms expressed in the heart [20]. Hypertrophic ligands such as insulin, insulin-like growth factor (IGF-1), endothelin-1, and LIF activate receptors on the cell membrane (i.e. tyrosine receptor kinase, G-protein coupled receptor, cytokine receptor). Activation of these receptors, by LIF for example, an interleukin 6 class cytokine produced by muscle that affects cell growth and development by signaling through the cell-surface type I cytokine receptor (CD126-gp130 complex), activates phosphoinositide 3-kinase (PI3K) to increase phosphatidylinositol (3,4,5) triphosphate (PIP_3) levels [12, 21-27]. PIP_3 recruits Akt via its PH domain to the plasma membrane where phosphoinositide-dependent protein kinase 1 (PDK1) and mTOR complex 2 (mTORC2) phosphorylate Akt at the T-loop Thr308 site and the hydrophobic motif Ser473 site, respectively [18, 21].

Full activation requires both sites to be phosphorylated, whereas singly phosphorylated Akt is only partially active [14]. Once activated, Akt dissociates from the plasma membrane and accumulates in the cytosol and nucleus, and recently found in mitochondria, where it is available to phosphorylate its downstream targets [14, 28, 29] (Scheme 1).

The involvement of Akt in the various cellular processes mentioned above is by the activation or inactivation of its downstream targets. Among Akt's downstream targets are tuberous sclerosis complex 2 (TSC2), 70-kDa ribosomal protein S6 kinase (p70S6K), mouse double mutant 2 (MDM2, or HDM2 in humans), and glycogen synthase kinase 3 (GSK3). The predominant mechanism for cell growth is through mTOR complex 1 (mTORC1), a critical regulator of translation initiation and ribosome biogenesis, of which the TSC2 tumor suppressor negatively regulates [18, 30]. mTORC1 activates S6K, which has been implicated as an important mediator in body and organ size regulation, most likely associated with increased rate of polyribosomal-mRNA bound translation [18, 31]. Akt-mediated phosphorylation inhibits TSC2, thus indirectly activating mTORC1 thereby enhancing protein synthesis through p70S6K [2, 18, 30]. Akt promotes cell survival by negatively regulating the function or expression of several pro-apoptotic Bcl-2 homology domain 3 (BH3)-only proteins through phosphorylation of MDM2 and GSK3 [30]. Phosphorylation of MDM2 (or HDM2 in humans) by Akt promotes nuclear translocation and degradation of p53, a transcription factor expressing BH3-only proteins [30]. The degradation of p53 by MDM2 also leads to a reduction in $p21^{Cip1}$ mRNA transcription, a cell cycle inhibitor, thus promoting cell cycle progression at the G1/S transition [14]. Also involved in cell survival is GSK3, which is normally active to inhibit

the prosurvival Bcl-2 family member myeloid cell leukaemia-1 (Mcl-1) through targeted-degradation phosphorylation [14, 30]. Additionally, downstream of Bcl-2 family members are caspase-9-initiated apoptosis cascades, whereby Bcl-2 prevents the processing of pro-caspase-9 into caspace-9 [30]. Overall, Akt phosphorylation inactivates GSK3 thereby preventing the processing of pro-caspase-9 and enhances stability of cell-cycle progression factors [2, 30]. While it is highly likely that cross-talk exists between Akt and other signaling pathways as regulators of these substrates, Akt is recognized to act on these substrates and possibly be protective for the heart.

Akt and Hypertrophy

The activation of the Akt signaling pathway has been suggested to be protective on the heart, as studies using overexpressed Akt or isoform specific knockout animal models portray Akt as a critical regulator for adaptive or maladaptive hypertrophy [18]. Cardiac-specific overexpression of activated PI3K (p110α), or the activated mutant, and myristoylated (membrane-targeted) Akt1 have all consistently demonstrated an increase in cardiac mass [5, 18, 22, 31, 32]. While overexpression of Akt is associated with cardiac hypertrophy, the duration of Akt activation determines the type of hypertrophy observed, as demonstrated in studies using inducible, cardiac-specific Akt1 transgenic mice where short-term Akt activation resulted in modest but reversible heart growth with preserved contractility, whereas long-term Akt activation resulted in excessive cardiac hypertrophy, contractile dysfunction, and interstitial fibrosis [5, 33]. Conversely, studies using Akt knockout mice models demonstrated impaired development and metabolism. Hearts of Akt1 deficient mice were found to have an exaggerated growth response to

pathological stimuli while being resistant to exercise-training induced hypertrophy, suggesting that Akt signaling actively suppresses signaling pathways that promote pathological hypertrophy [5, 22]. The same lab, using Akt2 deficient mice, demonstrated that Akt2 was dispensable for the development of hypertrophy, but necessary for the maintenance of normal cardiac glucose metabolism and for cardiomyocyte survival in response to injury [20]. Less relative to the cardiac field was a study on how Akt3 deficiency led to impaired embryo and postnatal brain development [32, 34]. Together these studies indicate the importance of Akt in proper development and cardiac function.

In addition to the extent of Akt activation, research studies suggest Akt localization also plays an important role in adaptive versus maladaptive cardiomyocyte growth and survival. Myristolated and constitutively active mutant Akt constructs tend to accumulate predominantly throughout the cytoplasm near the membrane, and to a lesser extent within the nucleus, in which Akt activation induced hypertrophy in cardiomyocytes [35]. However, normal physiologic Akt activation involves transient membrane association of which activated Akt eventually accumulates in the nucleus [21, 35, 36]. More recently, studies looking specifically at nuclear-targeted Akt activation showed profound anti-apoptotic activity without evidence of hypertrophic growth, but displayed an increase in the number of cardiomyocytes [35]. These studies further illuminate the understanding of the impact Akt signaling has on development and cardiac hypertrophy, in particular the duration of Akt activation and localization.

Novel Protein: PHLPP

Despite the amount of research on Akt activation, not much is known about Akt inactivation. Inactivation of Akt occurs through the dephosphorylation of Ser473 and Thr308 sites. Previous studies have identified two players involved in Akt inactivation: the protein phosphatase 2A (PP2A), which dephosphorylates Akt at Thr308, and PTEN (Phosphatase and Tensin homolog), which removes the activating PIP_3 signal thus preventing Akt phosphorylation and activation [18, 19, 28]. Until the recent discovery of the novel protein, PHLPP, the dephosphorylation of Akt at Ser473 remained elusive. This novel protein, named to reflect its domain structure: pleckstrin homology domain leucine-rich repeat protein phosphatase (PHLPP), was discovered by the Newton lab at UCSD by a database search for a sequence that contained a PH domain coupled to a phosphatase domain (Scheme 2) [28]. The ubiquitously expressed phosphatase, which has the highest levels in the brain, was earlier identified as SCOP (suprachiasmatic nucleus circadian oscillatory protein) and later determined to correspond to one of the PHLPP family members, PHLPP1β [28, 37, 38]. The PHLPP family is comprised of three members: PHLPP1α, PHLPP1β, and PHLPP2, with PHLPP1α and PHLPP1β being splice variants from the same gene located at chromosome 18q21.33 [28, 38, 39]. PHLPP2 is located at the chromosome 16q22.3 [38, 39]. PHLPP1 and PHLPP2 are identical in structure, however PHLPP1β and PHLPP2 contain an extra N-terminal Ras-association domain preceding the PH domain and the two isoforms share 58% amino identity in the PP2C domain and 63% amino identity in the PH domain [28, 38, 39]. The PP2C phosphatase domain is followed by a C-terminal type I PDZ-binding domain, crucial to the regulation of Akt dephosphorylation [38]. The molecular weight of PHLPP1α, PHLPP1β, and

PHLPP2 in *Mus musculus* is ~150kDa, ~180kDa, and ~170kDa respectively; in humans, the molecular weight of PHLPP is between 135 – 150kDa [28]. Cellular localization studies in numerous human cancer cell lines showed PHLPP1 and PHLPP2 present in the cytosolic, nuclear and membrane fractions [38, 39].

The PHLPP family are members of the protein phosphatase Mg^{2+}-activated (PPM) family of Serine/Threonine phosphatases. In addition to requiring Mg^{2+} or Mn^{2+} for its catalytic activity, PHLPP is dependent on the targeting of its PDZ binding motif for the regulation of Akt hydrophobic motif dephosphorylation and is not inhibited by traditional phosphatase inhibitors such as okadaic acid [28, 38, 39]. The Newton lab was able to show specific abolishment of Akt phosphorylation at Ser473 with no significant effect on Thr308 phosphorylation by PHLPP in transfected cells treated with or without okadaic acid [28]. Similarly, siRNA knockdown of PHLPP in lung cancer cells has shown that endogenous PHLPP catalyzes the selective dephosphorylation of Akt on its hydrophobic motif residue, Ser473, but not in the activation loop at Thr308 (Scheme 3) [28]. Although PHLPP1 and PHLPP2 were both shown to dephosphorylate the same residue on Akt, knockdown studies in cancer cells have shown differential regulation of the phosphorylation state of specific Akt isoforms, and in turn the phosphorylation state of different downstream targets [19, 38, 39]. The Newton lab performed siRNA knockdown and immunoprecipitation experiments in lung and breast cancer cells and showed PHLPP1 specificity for Akt2 and Akt3, whereas PHLPP2 has specificity for Akt1 and Akt3 [19, 38, 39]. This specificity can also be observed in Akt downstream substrates, specifically PHLPP1 affects GSK3α and HDM2, while PHLPP2 affects p27, and both PHLPP isoforms affect GSK3β and TSC2 [19, 38, 39]. However, studies done

in neonatal rat ventricular myocytes (NRVM) do not show such PHLPP isoform specificity towards Akt isoforms (Miyamoto unpublished data). Regardless, because phosphorylation of Ser473 may be the critical regulator of Akt activity, characterizing PHLPP and understanding its full physiological and biochemical pertinence to adult ventricular myocytes will be important for determining future research direction and potential therapeutic targets in heart disease treatment.

Choosing the appropriate Model System

The goal of studying signal transduction pathways involved in cardiac disease is to ultimately be able to treat human patients suffering from cardiomyopathy. Therefore, research and the extensive data collected should be from an appropriate animal model in which the information will be pertinent and can be extrapolated to how the human body would respond. Cardiomyocytes only represent about 30% of all heart cells, however they are the major contractile cells in the heart and most cardiac function disorders arise from problems with cardiac myocytes [40, 41]. To make pertinent the study of the effect of PHLPP on Akt in cardiomyocytes, adult mouse ventricular myocytes (AMVM) are the preferred model system to use, and have been used for the past 20 years as a model of the adult myocardium [42]. Neonatal rat ventricular myocytes (NRVM) are also a good system for studying cardiac function and are readily available and easily cultured, however due to the postnatal developmental stage of NRVM, AMVM correlate better to what is happening in the adult heart during hypertrophy [43, 44]. NRVM express fetal-genes (ex. β-myosin heavy chain (β-MHC)) and have very stable phenotype and contractile profile comparable to *in situ* hearts, whereas AMVM are terminally

differentiated, expressing a different set of genes (ex. α-MHC) and during ischemia-reperfusion differ from *in situ* hearts [8, 43]. Furthermore, compared to AMVM, NRVM have longer action potentials, heterogeneous cytosolic Ca^{2+} signals, weaker sarcoplasmic reticulum Ca^{2+} handling, and stronger sarcolemmal Ca^{2+} handling, with a significant contribution by the Na^{+}/Ca^{2+} exchanger [44]. In response to hypertrophy, adult cardiomyocytes increase in cell size only because they are unable to proliferate, whereas neonatal cells can still divide and adapt differently [45, 46]. Even the morphology between the two cardiomyocytes is different, where AMVM are rod-shaped and striated while NRVM are more confluent [42, 47]. To study the effects of PHLPP1 on Akt activity in adult cardiomyocytes, global *PHLPP1* null mice were generated in collaboration with the Newton lab. This unique strain of mice will allow us to study physiological levels of Akt activation, as opposed to other Akt mouse models where Akt activity and function are altered due to overexpression or constitutive activation of Akt.

Project Relevance

Given the importance of Akt in cell growth, metabolism, and survival, it is not surprising that much research effort has been made to determine its role in why, under the same signaling pathways albeit activated via very different stimuli, the heart will undergo either an adaptive or maladaptive hypertrophic response. Of particular interest is the question, will increasing Akt activation in the context of hypertrophy affect the heart to take on a more physiological or pathological hypertrophic phenotype. Despite the vast amount of knowledge available about Akt, it remains unclear whether increasing Akt activity during hypertrophy will increase angiogenesis and anti-apoptosis thereby

delaying the progression to heart failure, or if it will increase heart size in a way that progresses to heart failure even faster. We hope to contribute to answering these questions, however first we must understand the basic regulation of Akt by PHLPP. We hypothesize that removal of PHLPP1 will result in increased Akt phosphorylation at Ser473 after agonist stimulation in AMVM. Since much of the current research effort suggests Akt activation as potentially protective, perhaps removal of PHLPP1 will increase Akt activity and the physiological outcome will be hypertrophy without disease progression, increased angiogenesis, or inhibition of apoptosis. Correlating the events occurring at the individual cellular level to the organ as a whole will help elucidate the role of Akt in cardiac hypertrophy. To characterize removal of PHLPP1 in AMVM, we aim to: 1) isolate AMVM from WT and *PHLPP1* null mice and look at the baseline phenotype, 2) does removal of PHLPP1 affect Akt phosphorylation at Ser473 and Thr308 at baseline and following stimulation, 3) what effect will changes in Ser473 phosphorylation have on Akt activity and downstream target activation, and 4) will removal of PHLPP effect Akt compartmentalization. Being able to answer these questions can contribute to the understanding of the role of PHLPP in cardiomyocytes and gain insight to future experimental directions to contribute to understanding of the different signal transduction pathways differentiating adaptive from maladaptive cardiac hypertrophy.

Materials and Methods

All Buffers and Media are listed in Buffers and Media List (pg 48).

Gene Targeting and Generation of PHLPP1-Deficient Mice

A targeting vector replacing exon 4 of the *PHLPP1* gene with loxP-flanked exon 4 and FRT-flanked neomycin selection cassette was electroporated into mouse embryonic stem cells to generate *PHLPP1* null mice. Correctly targeted embryonic stem cells were identified by Southern blotting and subsequently injected into Black Swiss blastocytes to generate chimeric mice, which were bred with Black Swiss mice to generate heterozygous $PHLPP1^{+/flox}$ mice. Flox mice were bred with Protamine-Cre mice to generate heterozygous $PHLPP1^{+/-}$ mice. Finally, heterozygous $PHLPP1^{+/-}$ littermates were bred to generate true $PHLPP1^{-/-}$ mice [48, 49]. *PHLPP1* mice were genotyped by PCR on 3% agarose gels to confirm exon 4 deletion. Subsequent analysis of protein levels by Western blot was done to prove complete PHLPP1 protein removal with no changes to any other protein levels.

Isolating Adult Mouse Ventricular Myocytes

The isolation of adult mouse ventricular myocytes was adapted from published AFCS protocol [47].This procedure uses 8 – 12 week old mice.

Protocol Setup

All buffers and media were made up at least a day in advance, and kept no more than one week. Plates and/or chamber slides were coated with laminin (Table 3.1) at least 2 hours in advance.

The circulating water bath was set at 40.5˚C to allow the actual temperature of the heart during perfusion and digestion to be at 37˚C. The Langendorff apparatus was washed and equilibrated by continuously running Millipore water, followed by Perfusion buffer (Table 1.1a), through the entire apparatus. Priming the system with Perfusion buffer also eliminated air bubbles. The flow rate of the peristaltic pump was set to 3 ml/min.

Removal and Cannulation of the Heart

Mice were given heparin (40U) by intraperitoneal injection. Mice were anesthesized with isoflurane and 100% oxygen and cervically dislocated immediately before removal of the heart. The chest was cleaned with 70% ethanol. Hearts were collected in a 60-cm dish with perfusion buffer where extraneous tissue (thymus, lungs, adipose) could be removed. Within 1 minute, the heart was transferred to a clean 6-cm dish with perfusion buffer, cannulated just above the aortic valve, and the aorta was tied to the cannula with 6-0 surgical silk. Once cannulated, hearts were moved onto the Langendorff apparatus for perfusion and digestion.

Perfusion and Digestion of the Heart

Hearts were perfused with Perfusion buffer for 3-4 minutes at 3 ml/min to flush blood from vasculature and to remove extracellular calcium to stop contractions. Perfusion buffer was switched to Digestion buffer (Table 1.2) for 8 to 10 minutes at 3 ml/min until hearts were pale, swollen, soft, and exhibited a decrease in back-pressure. Once digestion was completed, hearts were cut from the cannula below the atria and placed in a 60-cm dish containing 2.5 ml Digestion buffer. Heart ventricles were gently teased apart into several small pieces, further dissociated by pipetting with two 1-ml

pipette tips, and collected into a 15 ml conical tube. Myocyte stopping buffer 1 (2.5ml, Table 1.3) was immediately added to the cells and pipetted up and down gently to ensure all cells came in contact with the stop buffer.

Calcium Reintroduction and Myocyte Plating and Culture

Cells were allowed to settle for 8-10 minutes by gravity. The supernatant was transferred to another 15 ml conical tube and centrifuged for one minute at 1000 rpm, while the gravity-pelleted cells were resuspended in 10 ml Myocyte stopping buffer 2 (Table 1.4). The supernatant of the centrifuged cells were aspirated off and the pelleted cells combined with the Myocyte stopping buffer 2 and cells suspension. Cells were passed through a 100-micron filter into a 6 cm dish and a series of calcium add-backs were performed every 4 minutes until reaching a final concentration of 1 mM $CaCl_2$. Cells were collected into a 15 ml conical tube and allowed to settle for at least 10 minutes by gravity. Cells were centrifuged for one minute at 1000 rpm, resuspended in Myocyte plating medium (Table 2.1), and plated onto laminin-coated dishes as appropriate. AMVM were plated for at least one hour to allow cells to adhere to the dishes. Plating media was replaced with Myocyte culture medium containing BDM (Table 2.2a). AMVM were left overnight in a 2% CO_2 incubator at 37˚C.

Stimulating and Harvesting Adult Mouse Ventricular Myocytes (whole extracts)

AMVM were treated with 10 nM LIF over a one hour time-course: Control (0 minutes), 5 minutes, 15 minutes, 30 minutes, 60 minutes. At the end of the time-course, cells were washed with cold PBS to stop stimulation and kept on ice.

PBS was carefully aspirated off. Depending on the density of cells plated, AMVM were harvested in 50 – 60 µl of Western buffer (Table 7.1). Myocytes were collected into microfuge tubes, and sonicated for at least one minute. Extracts were centrifuged for 15 minutes at 14,000 rpm at 4˚C and the supernatants were transferred to clean microfuge tubes. Protein concentrations were determined and samples were prepared for Western Blotting (see Protein Assay and Western Blotting Sample Preparation section).

Fractionation of Adult Mouse Ventricular Myocytes

All fractionation steps were done on ice. Buffers were prepared and kept on ice prior to harvesting (Table 7.1 – 8.3). Following stimulation, cells were harvested in 50 - 75 µl PBS with protease inhibitors cocktail (Table 8.3) and collected into chilled microfuge tubes. Cells were centrifuged at 2000 rpm at 4˚C. After removal of PBS, the pellet was resuspended in 30 - 40 µl Buffer C (Table 8.1 and 8.3) and incubated on ice for 15 minutes with tapping every 5 minutes. After incubation, cells were centrifuged at 5000 rpm at 4˚C and the supernatant, containing the cytosolic fraction, was collected into a clean, chilled microfuge tube. The pellet was resuspended again in 20 - 40 µl Buffer C and centrifuged at 5000 rpm at 4˚C. The supernatant was combined with the previously collected supernatant as the cytosolic fraction, and kept on ice. The pellet was resuspended in 50 - 80 µl RIPA buffer* and incubated on ice for 15 minutes, vortexing every 5 minutes. Both sets of microfuge tubes were centrifuged at 14,000 rpm at 4˚C and the supernatant was collected into clean, chilled microfuge tubes as cytosolic and nuclear fractions, respectively. Protein concentrations for cytosolic and nuclear fractions were

determined and samples were prepared for Western Blotting (see Protein Assay and Western Blotting Sample Preparation section).

*Due to the SDS in RIPA buffer interfering with the Bradford reagent during protein assay, Western buffer was substituted to lyse the nucleus.

Cell Size and Visualization

Cells were fixed with 4% paraformaldehyde (Table 9.1). FITC-conjugated wheat germ agglutinin (100μg/ml) was added to the cells and covered from light for 30 minutes. Cells were washed for 10 minutes twice with PBS/Triton-X and mounted with Hard Set Vectashield containing Dapi. Cells were visualized using an inverted fluorescence microscope at 10X objective. Cell area was measured using the ImageJ program (NIH).

Cell Staining and Visualization

Cardiomyocytes were prepared for immunocytochemistry as previously described [50]. AMVM were washed with cold PBS and fixed with either 4% paraformaldehyde (Table 9.1) for 15 minutes at room temperature or 1 ml ice cold methanol for 10 minutes at -20˚C. Only cells fixed with 4%-PF were permeabilized with 0.2% Triton-X (Table 9.2) for 5 to 10 minutes prior to being blocked in IC Block (Table 9.3) for 15 – 60 minutes at room temperature.

Primary antibody (1:500 α-actinin) was incubated overnight at 4˚C in a humidified chamber. Slides were washed 2-3 times with 0.2% Triton-X (Table 9.2). Secondary antibodies (1:4000 Alexa594-TRITC) were added to the cells for 1-2 hours

covered from light at room temperature. Slides were washed 2-3 times with 0.2% Triton-X before mounting with Vectashield containing Dapi (Antibody List Table 2.2).

Cells were viewed using a single capture microscope at 63X oil objective and analyzed using the MetaMorph program (Molecular Devices).

Protein Assay and Western Blotting Sample Preparation

Protein assay was performed following the Bradford protocol. Briefly, 5 µl of extract was added to 2 ml of Bradford reagent in a test tube. The absorbance of each sample was measured in duplicates at 595 nm using a spectrophotometer. Protein concentrations were determined against a standard curve. Samples (5 – 20 µg) were prepared in SDS loading buffer (Table 5.1), boiled for 5 minutes at 95˚C and centrifuged briefly prior to loading.

Kinase Assay

Whole cell extracts (40µg) were incubated in a microfuge tube containing Western buffer (Table 7.1), 50% slurry (50µl) of Protein A/G PLUS-Agarose beads (Santa Cruz Biotechnology, sc-2003), and monoclonal Akt (Table 3.1) overnight at 4˚C on a rotator. The following day, samples were spun down and the beads were washed 2-3 times with 50 mM Hepes, pH 7.6. After removing residual Hepes, 1X Kinase Reaction Buffer containing a GSK3 fusion peptide (Table 10.2) was added to the beads, and incubated at 30˚C for 60 minutes with gentle agitation every 10 minutes. Heated 5X SDS was added to the sample and boiled for 5 minutes at 100˚C. The samples were centrifuged and loaded onto a 4-12% Bis-Tris gel for Western Blotting (see below).

Western Blotting

Running SDS-PAGE gels

Samples were loaded onto Invitrogen NuPAGE Novex 4-12% Bis-Tris gels in MOPS Running buffer or 3-8% Tris-Acetate gels in TA Running buffer. Novex Sharp Pre-stained Standard from Invitrogen was used as the molecular weight marker. Gels were run for about 1.5 hour at 150 volts.

Protein Transfer

Before transfer, Millipore PVDF membranes were soaked in methanol for a couple seconds and allowed to equilibrate in Transfer buffer (Table 6.2). Proteins were transferred to PVDF membrane for 1 – 2 hours in Transfer buffer at 100 volts.

Immunodetection

Blots were blocked in 5% milk/TBS-T (Table 6.4) for 10 – 60 minutes. Blots were incubated overnight at 4˚C in primary antibody containing 5% BSA/TBS-T with 0.02% NaN_3 (Table 6.5) (Antibody List Table 1.1).

The following day, blots were washed 3 times in 1X TBS-Tween (Table 6.3) for 10 minutes. Blots were incubated in secondary antibody containing 5% milk/TBS-T (Antibody List Table 1.2) at room temperature for at least one hour. Blots were washed 3 times in 1X TBS-Tween for 10 minutes.

SuperSignal West Femto (Thermo Scientific) was used as the substrate for the HRP-conjugated secondary antibody. Blots were visualized using FluorChem Imaging software on Medium/Medium sensitivity using 2-3 minute exposure times. Band intensities were analyzed using the SpotDenso function.

Statistical Analysis

All band intensities were measured. To correct for loading, ratios of protein to loading control (total protein, GAPDH, α-tubulin) from the same blot were calculated. All time-point values were normalized to the WT Ctrl value. Data obtained under the same conditions were pooled and averaged. The standard deviation (S.E.) and standard error of the mean (S.E.M.) were calculated. Student's T-test using two-tailed distribution and two-sample equal variance (homoscedastic) was performed and a probability ≤ 0.05 was defined as significant.

Results

Generation of PHLPP1$^{-/-}$ null mice

To examine the function of PHLPP1 as a negative regulator of Akt signaling, viable *PHLPP1* null mice were generated in collaboration with the Newton lab at UCSD. Exon 4, which is contained by the *PHLPP1* gene, was deleted by homologous recombination using a targeting vector (Figure 1). Correctly targeted embryonic stem cells were used to generate chimeric mice, which were then used to generate germ line-containing heterozygous mice for the *PHLPP1*-targeted locus. Intercrosses of *PHLPP1*$^{+/-}$ mice yielded homozygous null mice at weaning at predicted Mendelian frequencies, indicating no developmental or perinatal lethality associated with loss of this gene [49]. Mice were genotyped using PCR analysis to confirm deletion of exon 4 in the targeted mice, indicating that a partial protein product for PHLPP1 was not possible. Lane 1 shows a visible *PHLPP1*$^{-/-}$ band at 486 base pairs (bp), whereas Lane 2 shows a visible *PHLPP*$^{+/+}$ band at 284 bp; Lane 3 shows *PHLPP*$^{+/-}$ bands visible at both 486 and 284 bp (Figure 2A). Western blot analysis of whole heart extracts showed a complete absence of PHLPP1 protein in *PHLPP1* null mice (KO lanes) with no compensatory changes in PHLPP2 or total Akt levels due to the loss of PHLPP1 protein (Figure 2B).

Isolation of Adult Mouse Ventricular Myocytes

Hearts from mice (8-12 weeks old) were used to isolate adult cardiomyocytes for the purpose of studying the effects of PHLPP1 removal on Akt signaling. Isolation and maintenance of cardiomyocytes in culture for 24 – 48 hours was achieved after months of practicing cannulation and learning the procedure. Good cannulation required hanging

the heart on the cannula right at the aortic arch without occluding flow into the coronary arteries. Successful isolation depended on proper perfusion and digestion times, the most critical being able to recognize when the heart was digested enough to minimize shearing but not so much that the cells were dying due to overdigestion. To determine the quality of individual cardiomyoctes for future experiments, isolated cardiomyocytes were stained with FITC-conjugated wheat germ agglutinin and visualized under an inverted microscope at 10X objective (Figure 3). Cells were also visualized for sarcomeric staining with α-actinin and nuclear staining with Dapi using a single capture microscope at 63X oil objective (Figure 3). Baseline characteristics such as cell size and shape were compared between age-matched WT and PHLPP1 KO mice. There was no significant difference in morphology or cell size between WT and PHLPP1 KO AMVM (Figure 4) (N_{Hearts}=2, N_{Cells}=1055). Overall, cells were determined viable for at least 24 hours and subsequent one-hour time course experiments were performed on isolated myocytes.

PHLPP1 removal increases phosphorylation of Akt at Ser473

Given that PHLPP is exclusive for Akt at its hydrophobic motif [19, 28, 38, 39], the effect of *PHLPP1* gene deletion on Akt phosphoryation at the Ser473 site in AMVM was investigated. Isolated AMVM, which were incubated overnight in serum-free media for recovery and return to baseline, were treated with 10nM LIF over a one-hour time course and the whole cell extracts were analyzed on Western blots. Whole cell extracts were immunoblotted with pAktS473 (60 kDa) and glyceraldehyde-3-phosphate dehydrogenase (GAPDH, 36 kDa), respectively, the latter as a loading control. As hypothesized, PHLPP1 removal resulted in an increased amplitude of Akt

phosphorylation at Ser473 at all time points compared to basal phosphorylation in WT mice. However, only at 15-minutes was there a significant increase (2-fold) in phosphorylation ($P \leq 0.05$). No change in the duration or timing of Akt Ser473 phosphorylation was observable, except for the difference in phosphorylation amplitude (Figure 5, $N_{WT}=17$, $N_{KO}=18$). Immunoblotting for total Akt confirmed that Akt is dephosphorylated over time rather than degraded, and quantification of phosphorylation normalized to total Akt is consistent with results normalized to GAPDH (data not shown). Thus, loss of the *PHLPP1* gene increases phosphorylation at Ser473, suggesting PHLPP1 protein normally functions as a negative regulator of Akt signaling.

PHLPP1 removal has no effect on phosphorylation of Akt at Thr308

To determine the specificity of PHLPP for Akt's hydrophobic motif, we investigated Akt phosphorylation at Thr308. Whole cell extracts from AMVM, serum-starved overnight and treated with 10nM LIF over a one-hour time course, were analyzed by Western blot. Extracts were immunoblotted for phosphorylated Akt at Thr308 (60kDa). Stimulation of WT or *PHLPP1*$^{-/-}$ AMVM with LIF produced a similar profile and magnitude of AktThr308 phosphorylation. No significant difference at any point was observed. There was no change in the overall profile of Akt Thr308 phosphorylation, even after careful quantification (Figure 6, N=9). These results confirm that the regulatory function of PHLPP1 protein is specific for the hydrophobic motif of Akt at Ser473 only, and does not normally function as a negative regulator of Thr308 phosphorylation.

PHLPP1 removal increases Akt kinase activity

Presumably, a change in phosphorylation levels of Akt in PHLPP null myoctes will correspond with a change in Akt activity levels as well. To investigate this hypothesis, WT and PHLPP KO AMVM were stimulated with or without 10nM LIF for 15 minutes and whole cell extracts (40μg) were immunoprecipitated for Akt. Activity was measured at 15 minutes post-LIF treatment because western blotting showed significant-potentiation of Ser473 phosphorylation in PHLPP1 KO myocytes compared to WT controls. Akt kinase activity was increased 30% in KO myocytes compared to WT myocytes at baseline (Figure 7, N=2). WT myocytes presented a 30% increase in kinase activity following LIF stimulation, whereas KO myocytes presented a 70% increase which is almost a two-fold increase in kinase activity after agonist stimulation. Thus preliminary data suggests removal of PHLPP1 not only results in an increased level of Ser473 phosphorylation in Akt after stimulation, but also corresponds to an increase in Akt kinase activity.

PHLPP1 removal on Akt downstream target phosphorylation

As there was a change in Akt activity upon loss of PHLPP1, the phosphorylation of Akt downstream targets in WT versus *PHLPP1* null mice were examined by Western blotting using whole cell extracts of isolated AMVM to correlate Akt activity with downstream phosphorylation. Myocytes were incubated overnight prior to stimulation with 10nM LIF. The phosphorylation of several Akt downstream targets were immunoblotted with phosphorylated TSC2 (200kDa), MDM2 (90kDa), p70S6K (70kDa),

GSK3α/β (46/51 kDa), and ERK1/2 (42/44 kDa). Due to the small amount of protein available, some of these downstream targets were undetectable. Given the limitations on looking at the Akt downstream targets, only phosphorylated GSK3α/β, MDM2, and ERK1/2, although not an Akt substrate, were quantified. In all three cases, there was no significant difference in protein phosphorylation at any given time. There was no difference in the phosphorylation profile of phosphorylated GSK3α/β between WT and PHLPP1 KO AMVM as quantified and normalized to WT ctrl (Figure 8, N=5). However, although the current data shows no significance, the phosphorylation profile of phosphorylated MDM2 seems to be slightly amplified in *PHLPP1* null mice with at least baseline phosphorylation leaning towards significant (0.085 and $P \leq 0.05$) (Figure 9, N=11). The phosphorylation profile of the Map kinase pathway ERK1/2 was also determined in WT and PHLPP1 KO AMVM. This was investigated because of the possibility of cross-talk between removal of PHLPP and other signaling pathways. We found that there was no significant difference in Erk activation in WT and PHLPP1 KO AMVM treated with LIF (data not shown). Overall, the data remains inconclusive as to whether removal of PHLPP1 protein increases Akt downstream target activation as phosphorylation states of these targets can be affected by signaling pathways other than Akt and Erk.

Fractionation of Adult Mouse Ventricular Myocytes

Several studies have distinguished the function of cytsolic versus nuclear Akt and the role each may have on the development of adaptive versus maladaptive hypertrophy [21, 35]. To eventually address the role of Akt and PHLPP localization, it is important to

determine if PHLPP1 removal would affect the movement of Akt. Isolated AMVM were stimulated with 10nM LIF over a one-hour time course and separated into cytosolic and nuclear fractions. Due to the sensitivity and difficulty of this protocol, protein concentrations tended to be low, and each fractionation yielded enough protein extract to run one set of Western blots. Cytosolic fractions from WT and PHLPP1 KO myocytes were run together on one gel, and nuclear fractions were run together on a separate gel. Controls for cytosolic fractions were blotted with RhoGDI (28kDa) and the nuclear fractions were blotted with LaminA/C (70kDa). Western blotting demonstrated clean fractionation of the cytosol from the nucleus (Figure 10, 11). *PHLPP1* null mice exhibited a shift resulting in earlier Akt Ser473 phosphorylation in both cytosolic and nuclear fractions as compared to WT (Figure 10, 11). Previous blots of whole cell extracts showed a peak in Akt Ser473 phosphorylation at 15 minutes followed by gradual dephoshorylation and return to almost baseline phosphorylation levels by 60 minutes. Yet fractionated extracts from *PHLPP1*$^{-/-}$ myocytes peaked at 5 minutes followed by a much slower dephosphorylation, and eventually returning to baseline phosphorylation levels by 60 minutes. The differences in phosphorylation profile between whole cell and fractionated extracts can be explained by relatively spread-out time-points and it is possible that we missed vital incidents occurring in between. So far as we can conclude, the phosphorylation profile of both cytosolic and nuclear Akt Ser473 parallel each other, which suggests that PHLPP affects Akt in both compartments of the cell.

Schemes and Figures

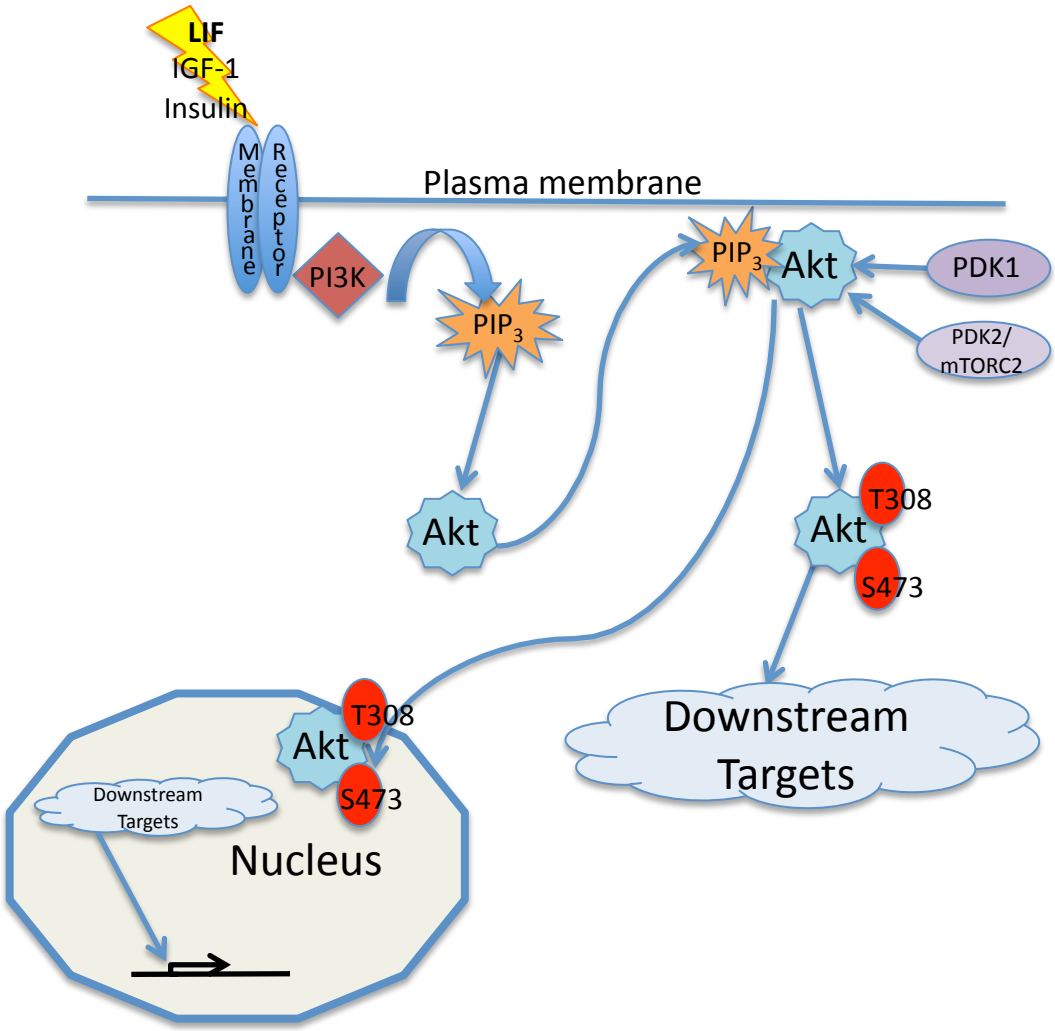

Scheme 1: Akt Signaling Pathway Hypertrophic ligands activate receptors on the cell membrane to activate PI3K, which increases PIP_3 levels. PIP_3 recruits molecules with PH-domains to the plasma membrane, including Akt. Akt gets phosphorylated at Thr308 and Ser473 by PDK1 and PDK2, respectively. Activated Akt accumulates in the cytosol and nucleus and phosphorylates its downstream targets.

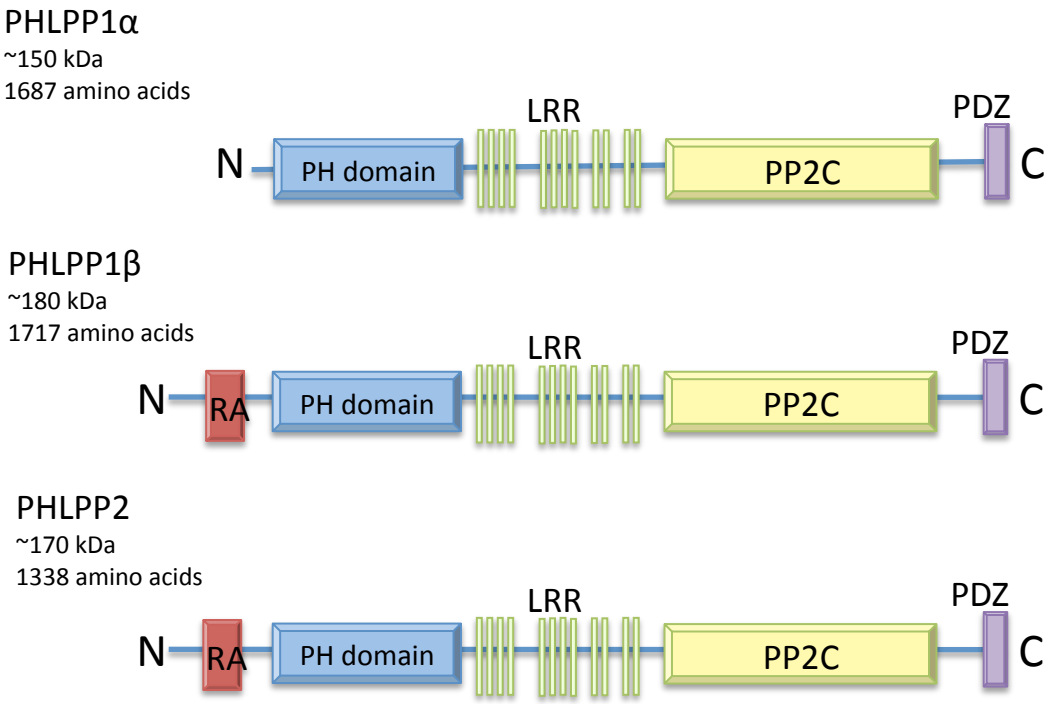

Scheme 2: PHLPP Isoform Schematic PHLPP1α and PHLPP1β are splice variants of the same gene. PHLPP1 and PHLPP2 are identical in structure located at chromosome 18q21.33 and 16q22.3, respectively. However, PHLPP1β and PHLPP2 contain an extra N-terminal Ras-association domain (RA).

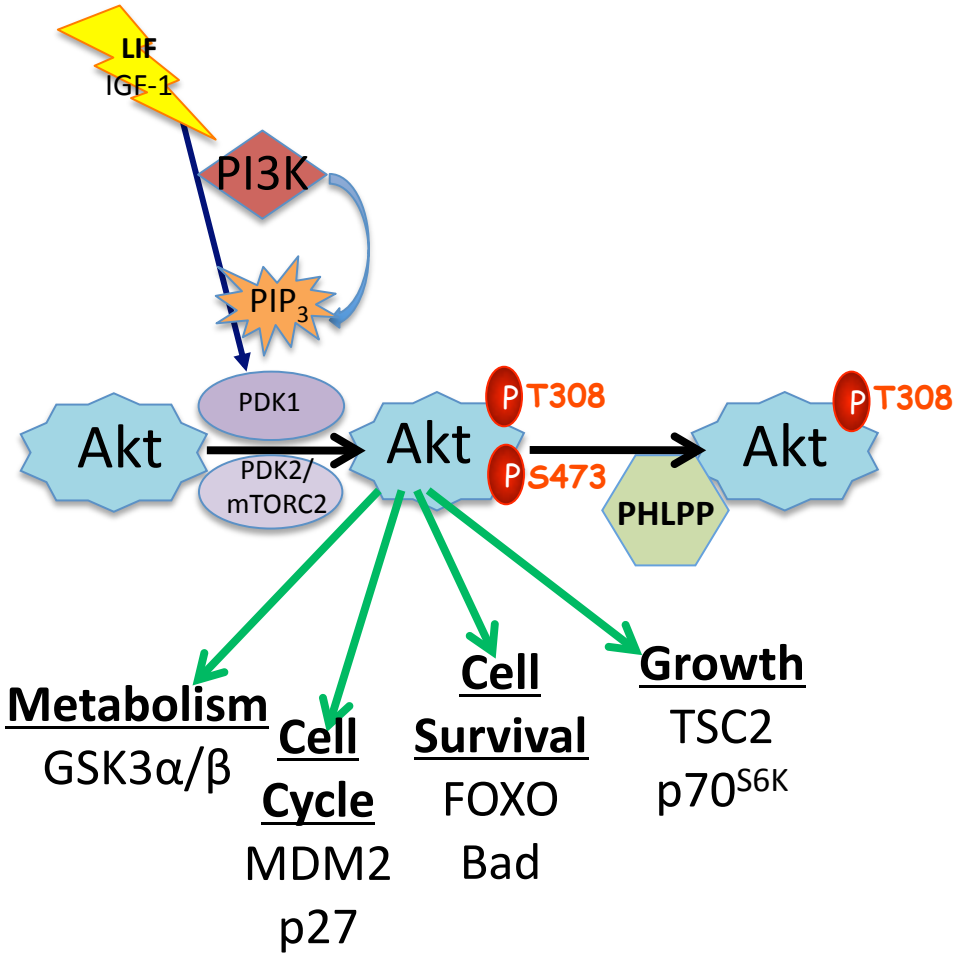

Scheme 3: PHLPP Signaling Pathway Akt is fully active when it is phosphorylated at both Thr308 and Ser473 sites. PHLPP specifically dephosphorylates Akt at the Ser473 site.

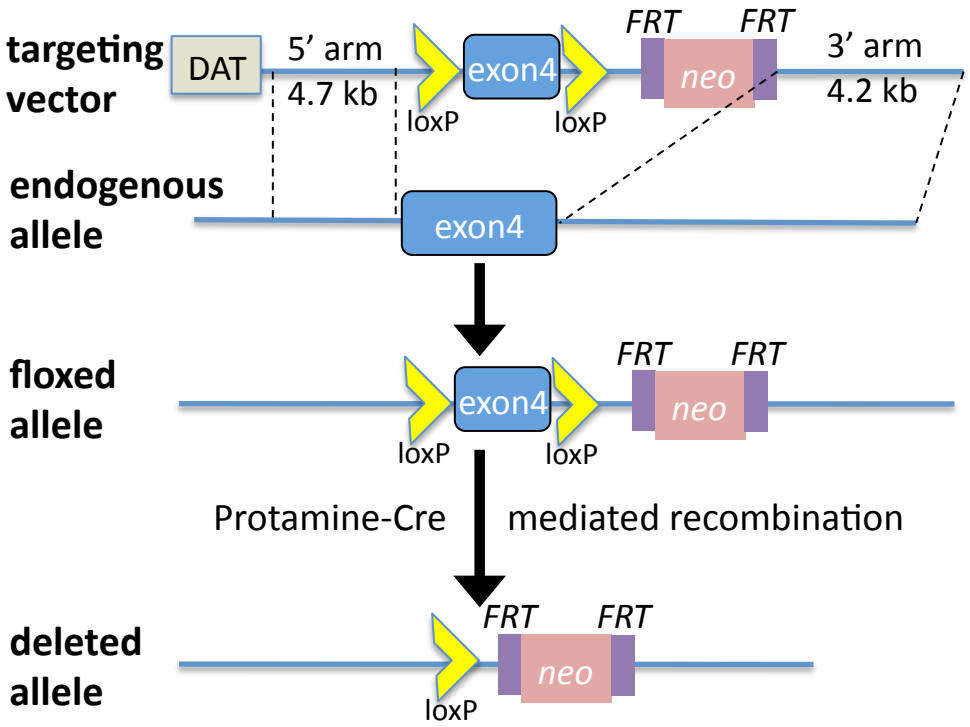

Figure 1: Gene-targeting schematic of PHLPP1 knock-out mice.
Schematic of the *PHLPP1* genetic locus in the mouse and the targeting vector that was used to replace exon 4 in embryonic stem cells.

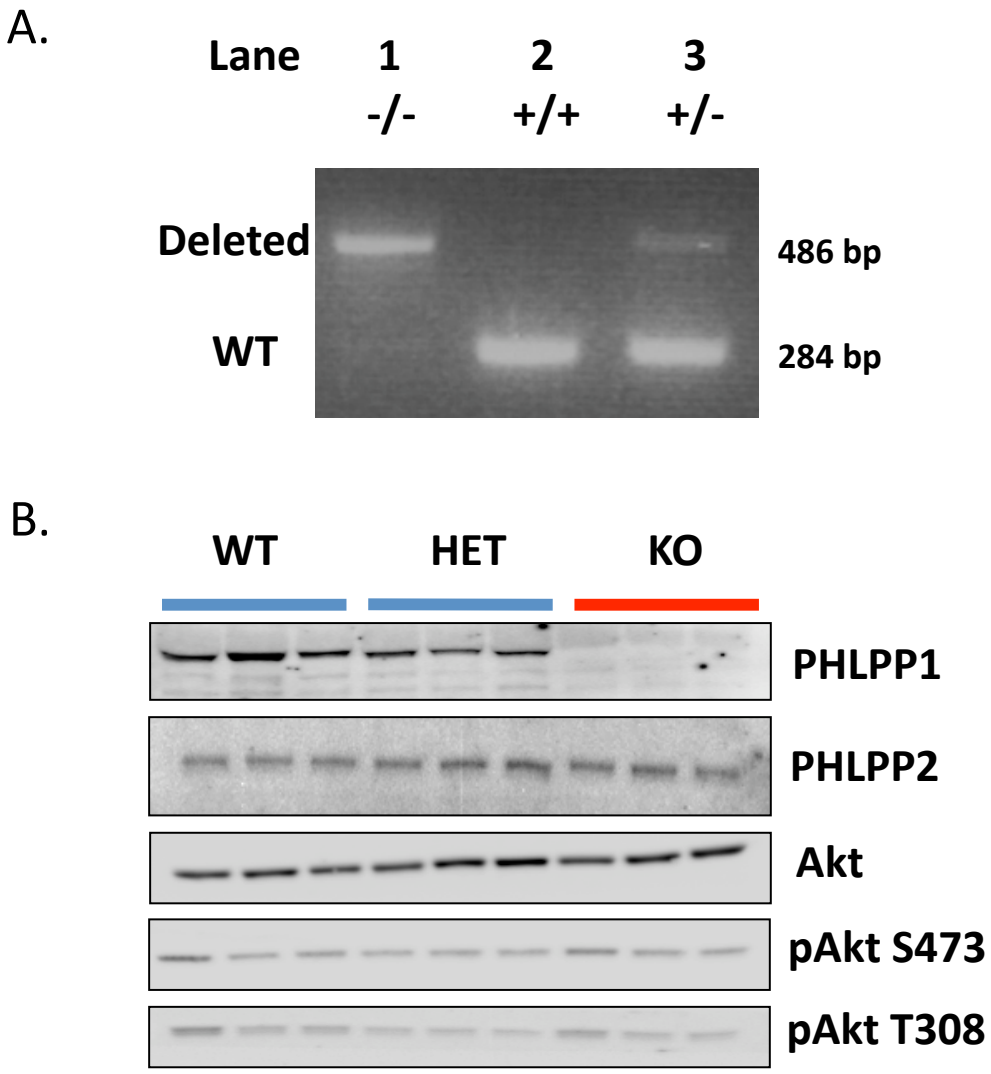

Figure 2: Targeted disruption of PHLPP1 **(A)** PCR data showing deletion of exon 4 in *PHLPP1* gene-targeted mice. **(B)** Homogenized whole heart extracts (100µg)of wild-type (WT), Heterozygous (HET), and PHLPP1 gene-targeted mice (KO) were analyzed by Western blot for PHLPP and Akt protein.

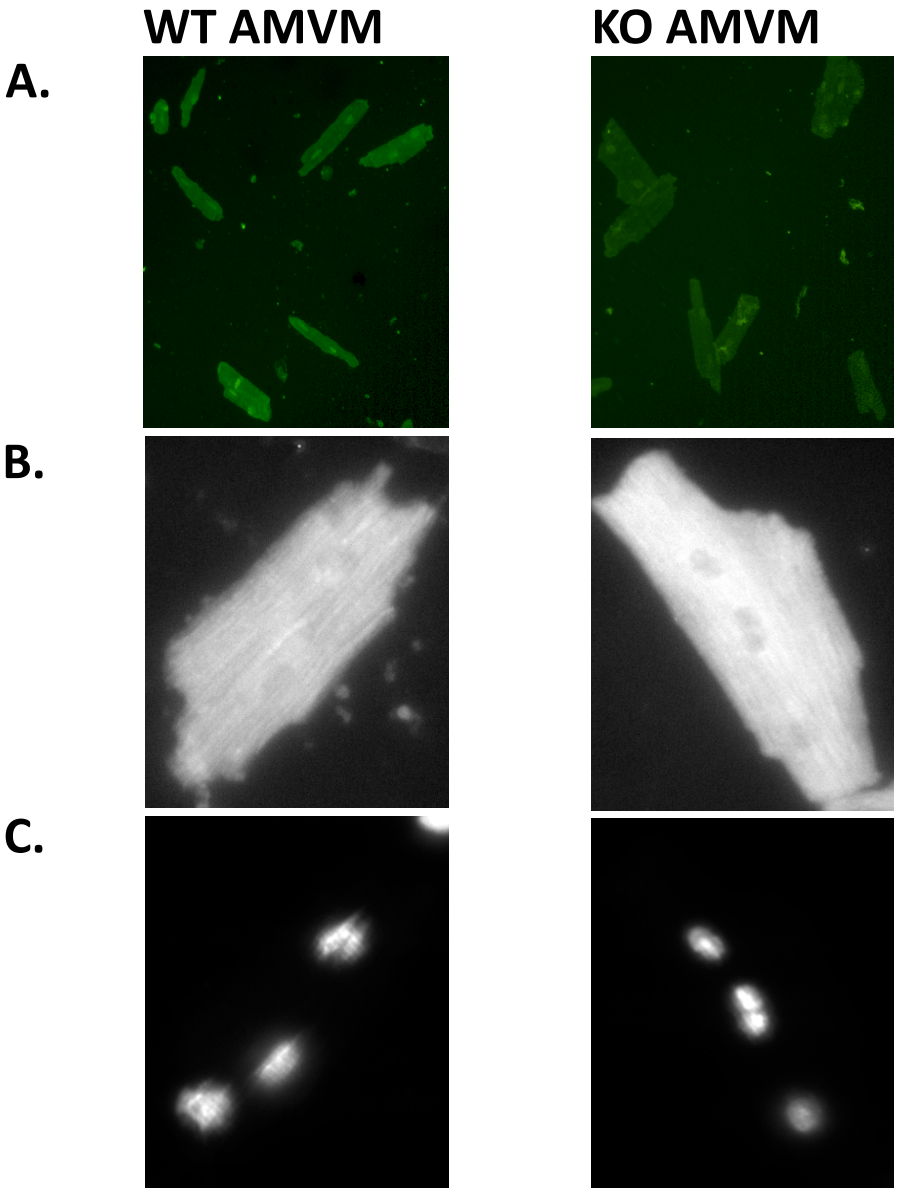

Figure 3: Visualization of isolated AMVM **(A)** Isolated AMVM stained with FITC-conjugated wheat germ agglutinin visualized using an inverted fluorescence microscope at 10X objective. **(B)** Isolated AMVM stained with α-actinin (1:500) to visualize sarcomeres or **(C)** Dapi for nuclear staining using a single capture microscope at 63X oil.

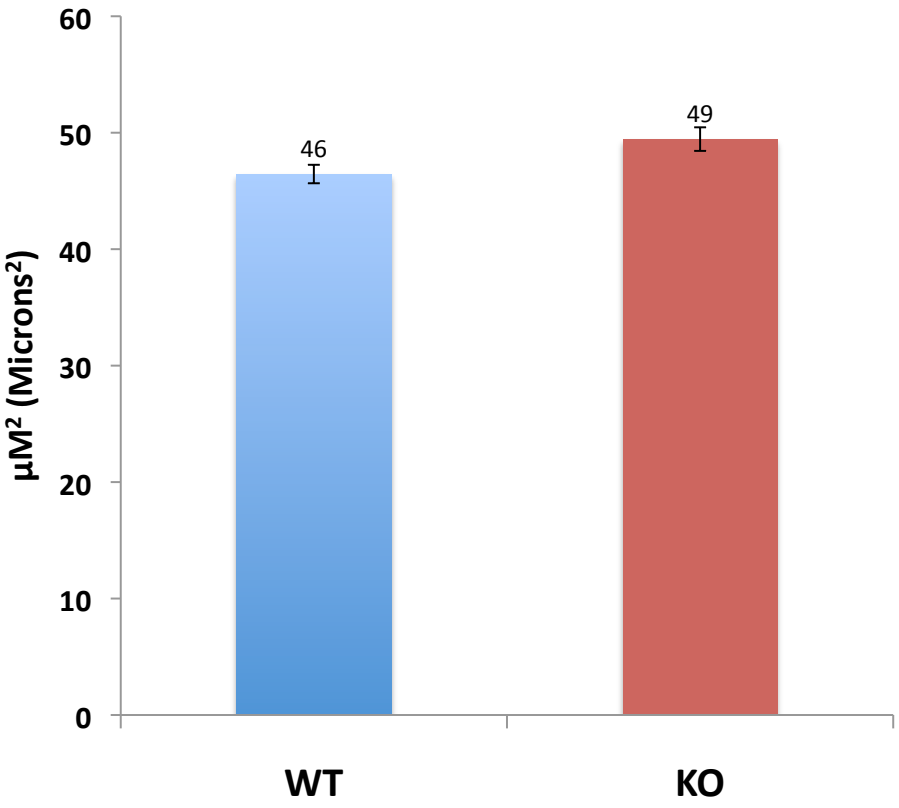

Figure 4: Cell size measurement Isolated cardiomyocytes were stained with FITC-conjugated wheat germ agglutinin. Individual myocyte cell areas were measured using ImageJ. Bar graph of averaged cell size (N=1055 cells).

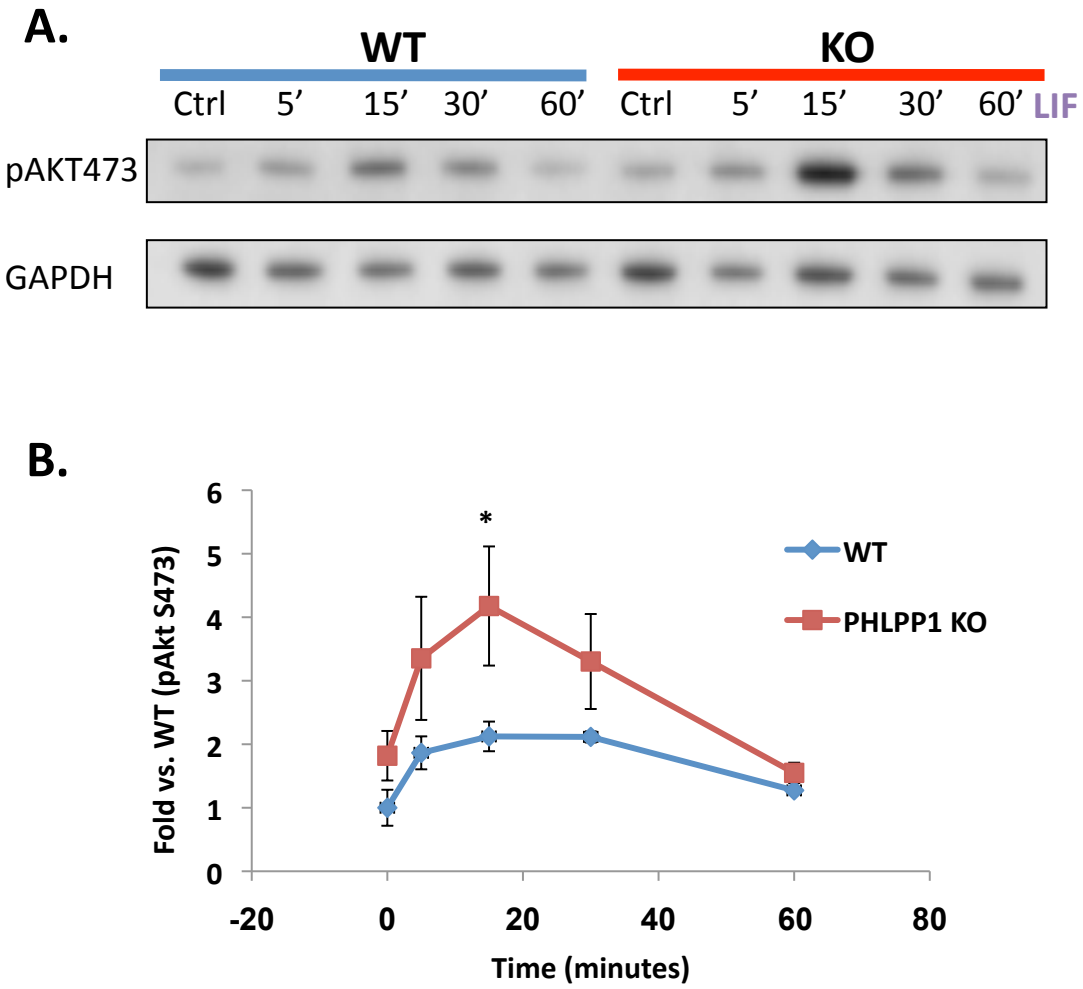

Figure 5: PHLPP1 removal increases phosphorylation of Akt at Ser473 after LIF stimulation in AMVM (A) Representative western blot of Akt phosphorylation at Ser473 from whole cell extracts of isolated AMVM (5µg) treated with 10nM LIF over a one-hour time course. **(B)** Graph of the average fold increase of pAkt473 as normalized to WT Ctrl (N_{WT}=17, N_{KO}=18). * indicates significance by Student's T-test ($P \leq 0.05$).

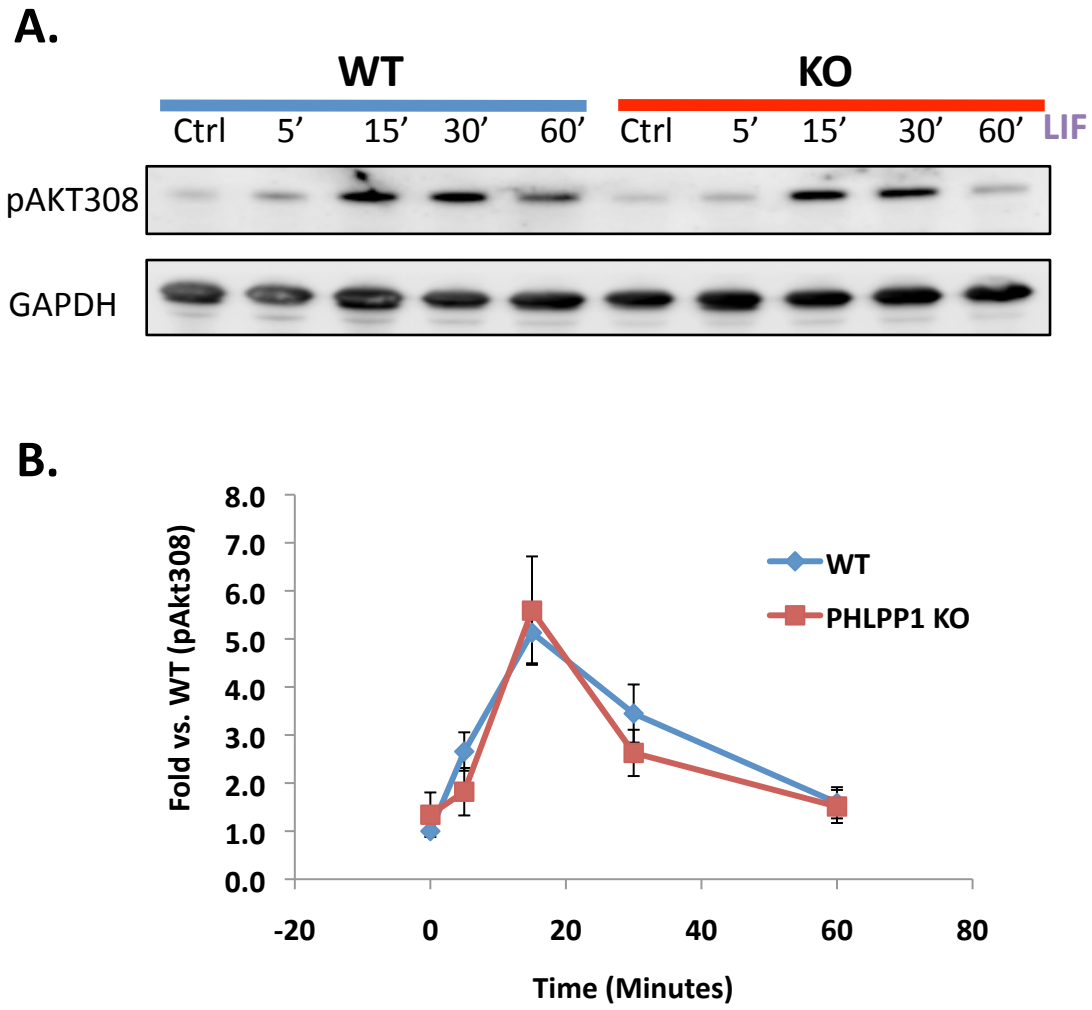

Figure 6: PHLPP1 removal has no effect on Akt phosphorylation at Thr308 after LIF stimulation in AMVM (A) Representative western blot of Akt phosphorylation at Thr308 from whole cell extracts of isolated AMVM (10µg) treated with 10nM LIF over a one-hour time course. **(B)** Graph of the average (N=9) fold increase of pAkt308 as normalized to WT Ctrl.

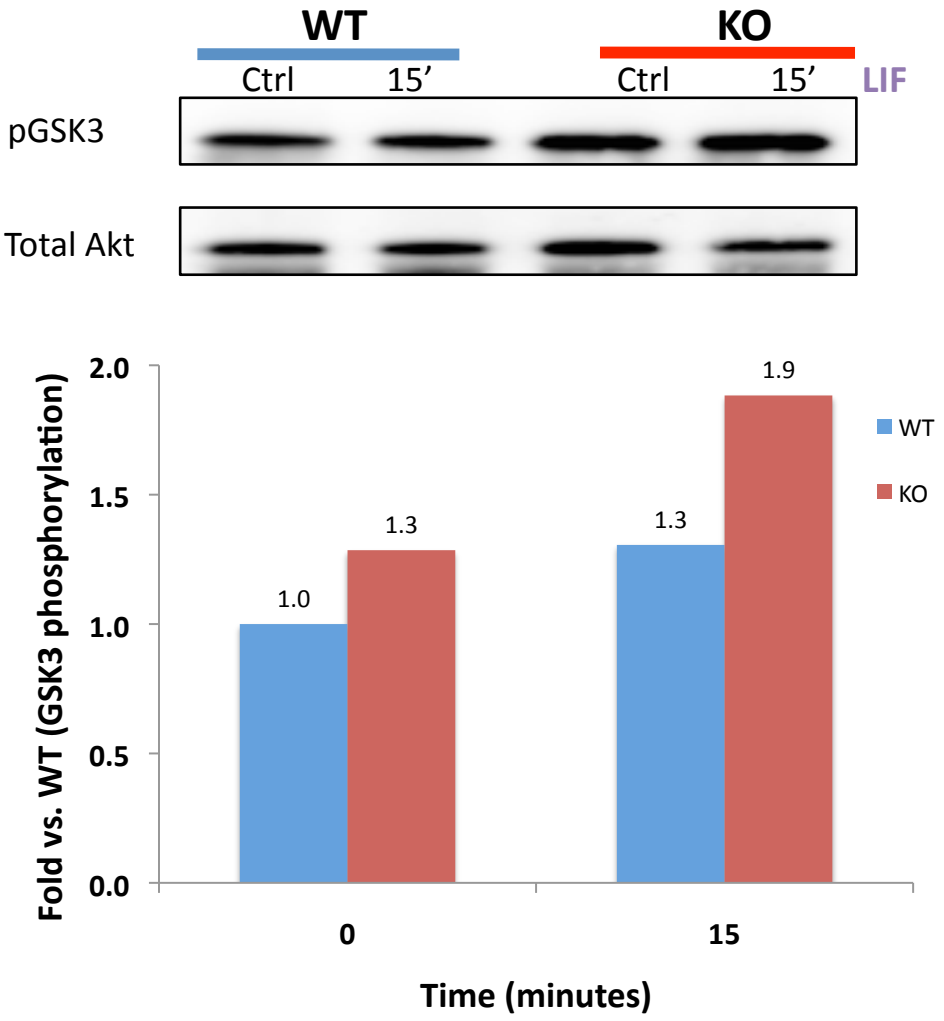

Figure 7: Loss of PHLPP1 results in increased Akt kinase activity after LIF stimulation in AMVM Akt from control and 15-minute LIF-stimulated cardiomyocytes were immunoprecipitated and subjected to a kinase assay using a GSK peptide substrate. At baseline, Akt from KO AMVM exhibited a 30% increase in kinase activity compared to that of WT AMVM (N=2). Comparing within genotypes, WT myocytes exhibited 30% increase whereas KO myocytes exhibited 70% increase in kinase activity after LIF stimulation, a near two-fold increase in kinase activity after agonist stimulation.

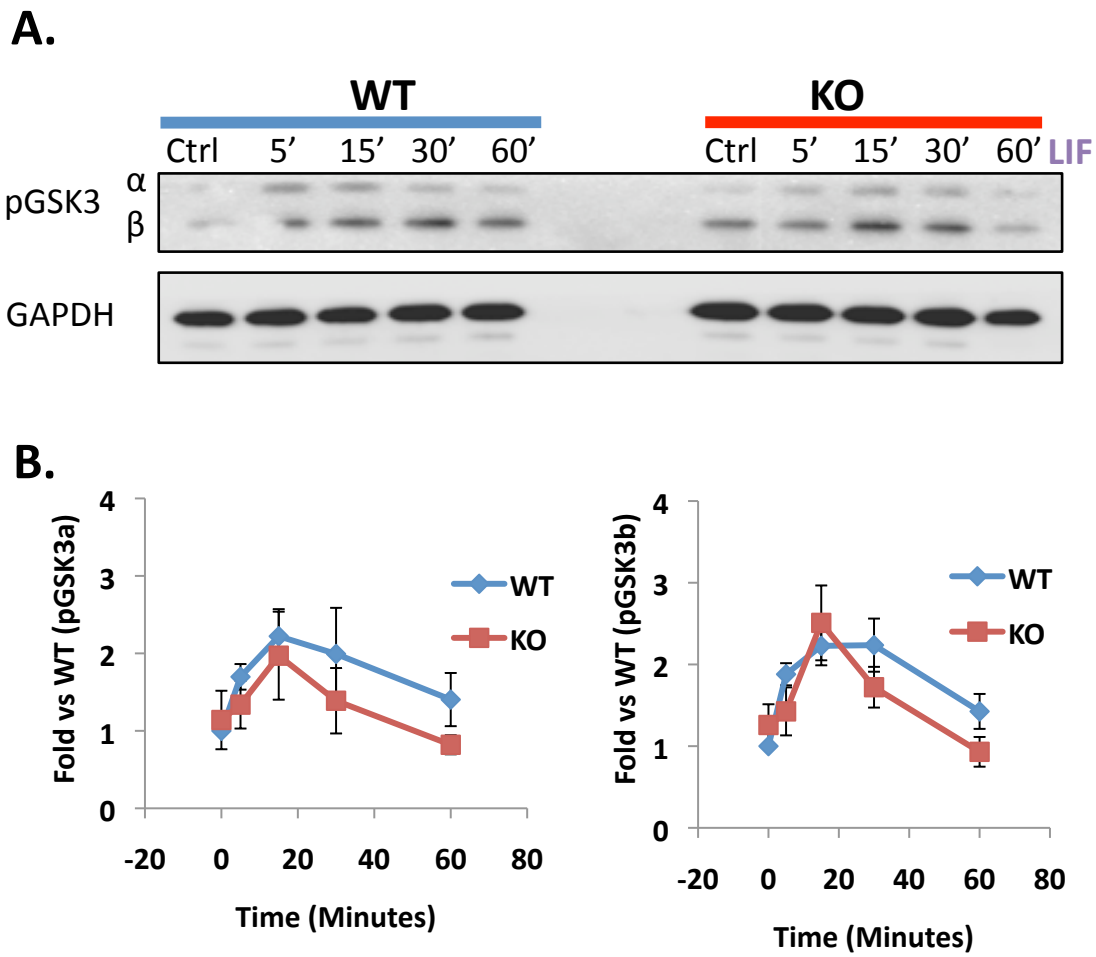

Figure 8: PHLPP removal has no effect on GSK3α/β phosphorylation after LIF stimulation in AMVM **(A)** Representative Western blot of GSK3α/β phosphorylation from whole cell extracts of isolated AMVM (5µg) after 10nM LIF stimulation. **(B)** Graph of the average (N=5) fold increase of pGSK3α/β as normalized to WT Ctrl.

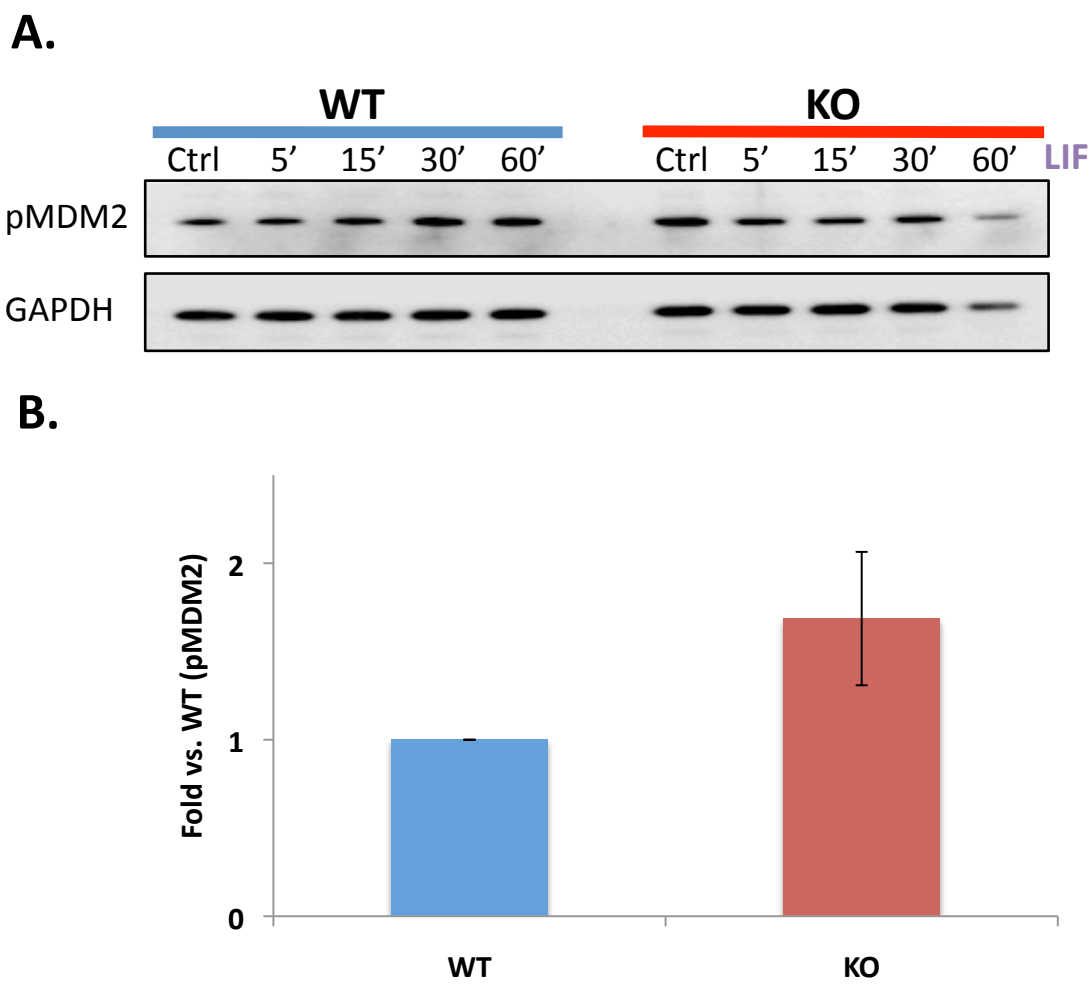

Figure 9: PHLPP removal slightly increases MDM2 phosphorylation at baseline in AMVM **(A)** Representative Western blot of MDM2 phosphorylation from whole cell extracts of isolated AMVM (5µg) after 10nM LIF stimulation. **(B)** Graph of the average (N=11) fold increase of pMDM2 as normalized to WT Ctrl at baseline. At baseline, the difference between WT and KO myocyte phosphorylation levels is leaning towards significance (P = 0.085).

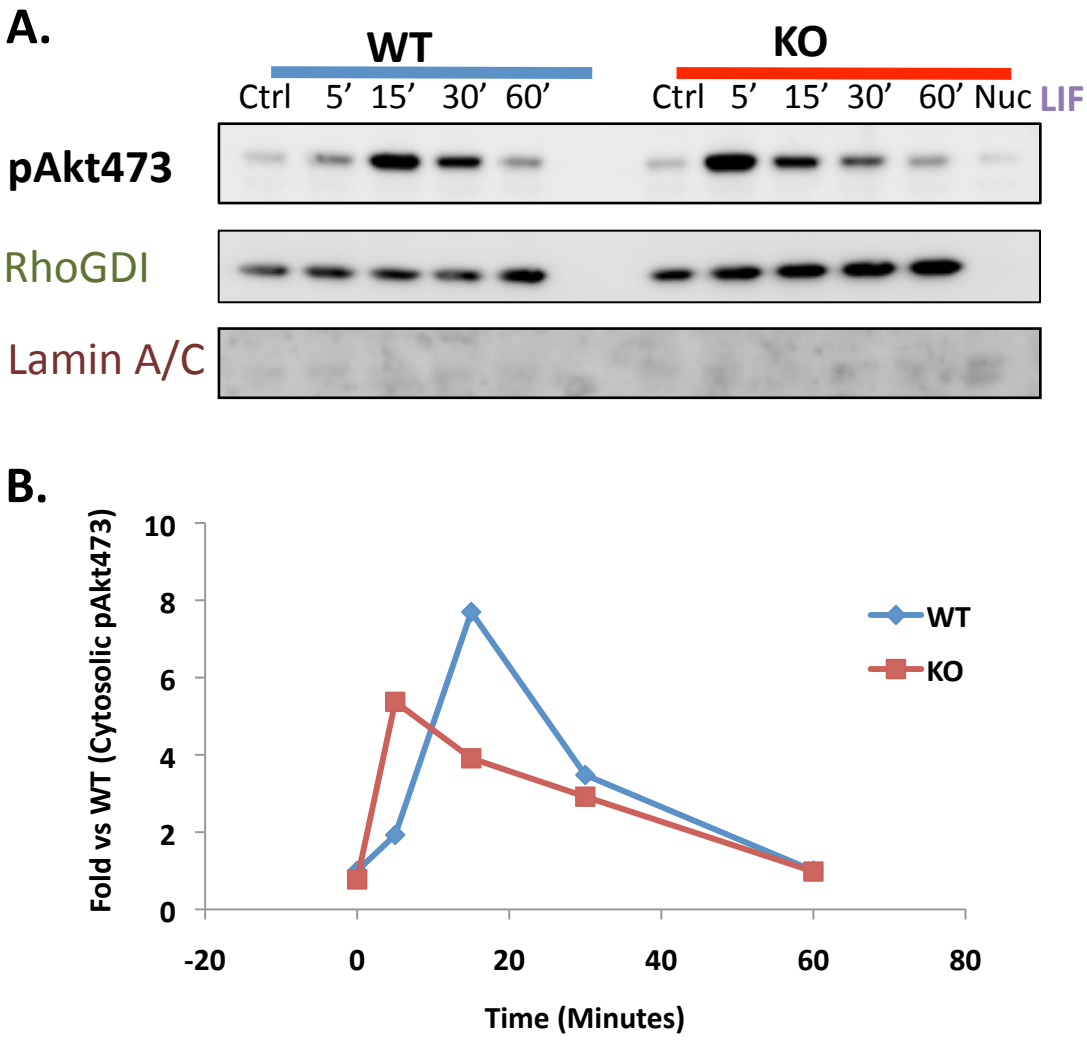

Figure 10: Effect of PHLPP1 removal on cytosolic Akt phosphorylation in AMVM after LIF stimulation **(A)** Representative western blot of AMVM cytosolic fraction (10µg) stimulated with 10nM LIF. Control blots shown for the cytosolic marker, RhoGDI, and nuclear marker, LaminA/C. **(B)** Graphs of the average (N=2) fold differences as normalized to WT Ctrl shown.

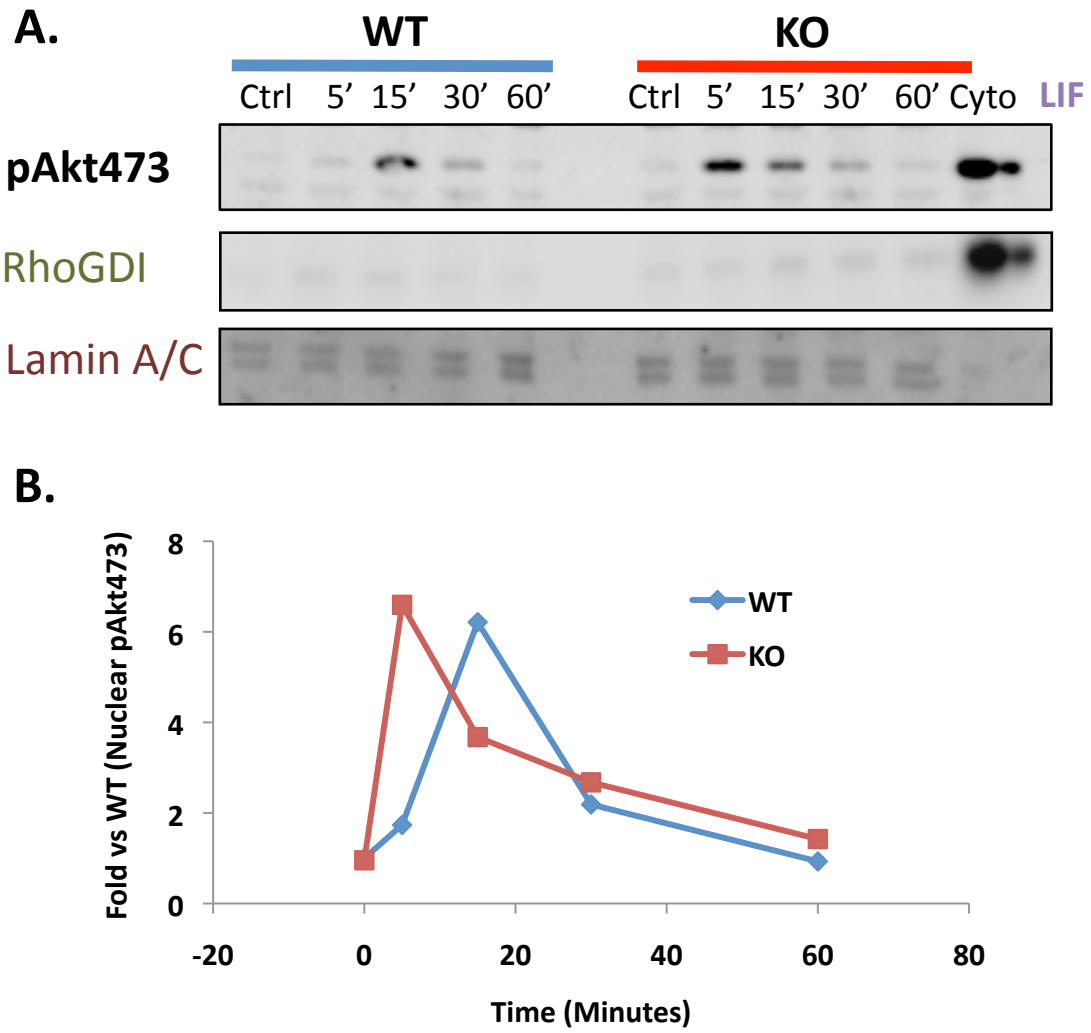

Figure 11: Effect of PHLPP1 removal on nuclear Akt phosphorylation in AMVM after LIF stimulation **(A)** Representative western blot of AMVM nuclear fraction (15µg) stimulated with 10nM LIF. Control blots shown for the cytosolic marker, RhoGDI, and nuclear marker, LaminA/C. **(B)** Graphs of the average (N=2) fold differences as normalized to WT Ctrl shown.

Discussion

Our lab is interested in the activation of Akt and its role in the progression of cardiac hypertrophy. PHLPP is a ubiquitously expressed phosphatase that dephosphorylates Akt specifically at Ser473 leading to inactivation of Akt. To characterize the effect of PHLPP on Akt signaling in the heart, we collaborated with the Newton lab to generate *PHLPP1* knockout mice. *PHLPP1*$^{-/-}$ or *PHLPP1*$^{+/-}$ mice did not show embryonic, postnatal, or adult lethality. Western blot analysis confirmed complete PHLPP1 loss with no changes in PHLPP2 or total Akt levels. Given the successful generation of PHLPP1 knockout mice, we wanted to study Akt signaling at the cellular level, thus subsequent experiments were done *in vitro* on adult mouse ventricular myocytes (AMVM).

This project focuses on the initial characterization of PHLPP removal on Akt in adult cardiomyocytes. Being able to discern cellular effects of cardiomyocytes from other cell types will serve as a platform for future studies involving the whole heart and PHLPP's involvement in cardiac hypertrophy. Myocytes from 8 – 12 week old mice were isolated and stained for visualization to compare cell phenotypes from wild-type (WT) and PHLPP1 KO cardiomyocytes. The isolation of stable adult cardiomyocytes required months of optimization due to the cells' sensitivity to the quality of cannulation, enzyme digestion activity, perfusion temperature, and stability of buffers. Sterility of the apparatus and timing of each step also influenced the viability of the isolated cardiomyocytes. Despite these obstacles in obtaining the cells, practice and experience was rewarded with successful isolation and maintenance of quality AMVM for 24-48 hours in culture. Cardiomyocytes incubated overnight in serum-free media displayed no

overt phenotypical differences. Isolated cardiomyocytes from WT and KO mice were rod-shaped, multi-nucleated, and had clear striations when stained with α-actinin. Since Akt is involved in cell growth and protein synthesis and studies in mice with overexpressed or constitutively active Akt have demonstrated increased cardiac mass, we investigated the removal of PHLPP1 on cardiomyocyte cell size [5, 12, 18, 22, 31, 32]. Upon measuring cell area, PHLPP1 null myocytes were not significantly different from WT cells. The lack of significant difference in individual cell size is consistent with the comparison of total heart weight to body weight ratios between WT and KO mice which show no baseline phenotype (Purcell, data unpublished).

Earlier studies by Brognard et al in cancer cells demonstrated that PHLPP dephosphorylates Akt specifically at Ser473 with minimal effects at Thr308. Similarly, we found that PHLPP1 removal increases the amplitude of phosphorylation of Akt at Ser473 in adult cardiomyoctes, without changing the phosphorylation profile of Akt at Thr308. Our data about PHLPP's effect on Akt phosphorylation in AMVM is the first study done in cardiac myocytes and supports our hypothesis. Given that PHLPP is an Akt phosphatase, removal may result in prolonged Ser473 phosphorylation following agonist stimulation. Despite the increased amplitude in phosphorylation, the duration of Akt activation did not change between WT and KO myocytes following LIF stimulation. This could be a result of compensatory actions by PHLPP2 or other unidentified Ser473 phosphatase(s). Notably, there was no up-regulation of PHLPP2 (Figure 2), the more sensible explanation is that PHLPP1 is only required when there is high levels of Akt activity. Lastly, there could also be other mechanisms regulating Akt de-phosphorylation by upstream or downstream substrates. Regardless of the mechanism, this transient

phosphorylation state of Akt represents a more physiological activation compared to other *in vivo* Akt models using overexpressed or constitutively active Akt [5, 18, 22, 31-33]. The PHLPP KO mouse represents a model of Akt activation at physiological levels and will provide more applicable data towards understanding Akt activation of downstream targets and subsequent involvement in cardiac hypertrophy.

The widely available literature on Akt correlates increased phosphorylation of the kinase with increased activity of the signaling pathway [14, 18, 21, 28, 29]. With the encouraging results of increased Akt phosphorylation at Ser473 in the absence of PHLPP1, we performed an *in vitro* kinase assay to determine Akt activity. Although data is preliminary, we found increased Akt activity in PHLPP KO mice at baseline and following LIF stimulation compared to WT controls. Since an increase in Akt activity usually corresponds to an increase in target activation, we investigated the phosphorylation of several downstream signaling pathways. The phosphorylation levels of MDM2, GSK3, and ERK were investigated following LIF stimulation in WT and KO myocytes. MDM2 phosphorylation levels showed a trend towards significance at baseline, yet GSK3 phosphorylation levels were not significant between WT and KO myocytes after LIF stimulation. Other than Akt signaling, MDM2 stabilization is regulated by various factors (i.e. the tumor suppressor ARF, MdmX (or Mdm4), and HAUSP) [54]. In the same respect, GSK3 is constitutively active and phosphorylation at certain Ser/Thr residues by kinases such as p38 MAPK, AGC, p90S6K decrease its activity [55]. The efficiency of cross-talk between Akt and the multitude of signal transduction pathways on a particular substrate remain unaddressed and could be a factor in discrepancies seen in target phosphorylation. Furthermore, there may be alternative

splicing, post-translational or feedback regulations that ensure a constant amount of protein at any given moment that counteracts effects of increased Akt activity.

Akt and ERK, a mitogen-activated protein kinase, are both involved in cell survival and proliferation and are activated by the JAK/STAT pathway (Janus-activated kinase/signal transducers and activators of transcription), growth factors, and hormones [51-53]. To determine the specificity of PHLPP on Akt, we investigated the phosphorylation level of ERK after LIF stimulation and found no significant differences between WT and KO myocytes (data not shown). Though these results suggest high specificity of PHLPP for Akt, it would be presumptuous to make such a claim since pathways other than ERK have not been investigated. Ultimately, in regards to direct activity, PHLPP1 removal increases Akt activity at baseline and following LIF stimulation in AMVM.

Apart from the duration and amplitude of activity, Akt localization has been found to play an important role in the regulation of cardiac hypertrophy and apoptosis [21, 29, 35, 36]. To see if PHLPP1 removal affected Akt compartmentalization and activation, we stimulated WT and KO myocytes with 10nM LIF and fractionated the cells into cytosolic and nuclear compartments. The protocol allows us to assume, in terms of Akt, that the cytosolic fraction contains membrane-associated and cytoplasmic Akt without contamination from other compartments such as mitochondria and nucleus. Likewise, the nuclear fraction should contain only nuclear-accumulated Akt. Surprisingly, myocytes from *PHLPP*$^{-/-}$ mice showed a peak in Akt Ser473 phosphorylation at 5 minutes, rather than at 15 minutes as was observed in whole cell lysate western blots. This observation was made in both cytosolic and nuclear fractions.

Notably, the phosphorylation profile of Akt at Ser473 in WT AMVM did not change in comparison to whole cell lysate western blots. In both WT and KO AMVM, Akt phosphorylation was not sustained and followed a gradual dephosphorylation pattern. At this time, it is unclear why this discrepancy in the phosphorylation peak is seen between whole cell extracts and fractionation data. It could be that in fractionating the cells, Akt in other cellular compartments are not included in the analysis. Due to the limited range of time points studied, we could also be missing other incidents of Akt phosphorylation occurring between the time points we use. There is much that still needs to be done to understand if PHLPP1 has an affect on Akt localization and translocation. Currently we are optimizing conditions to visualize Akt movement and PHLPP in cardiomyoctes. Our data indicates that PHLPP1 removal results in an earlier peak in Akt phosphorylation at Ser473 after LIF stimulation in both cytosol and nuclear fractions of AMVM which may lead to greater Akt activity or an enhanced response to extracellular stimuli. This needs to be further investigated.

Despite the many unanswered questions, our data provides the first characterization of PHLPP1 removal in adult mouse ventricular myocytes. We deleted exon 4, the gene encoding for PHLPP1, to generate viable *PHLPP1*$^{-/-}$ mice. Comparing myocyte phenotypes, we concluded that there were no overt changes to morphology, organization, or cell size. We confidently determined that removal of PHLPP1 in AMVM increases Akt phosphorylation at Ser473 with minimal changes to the phosphorylation at Thr308. In studying the consequence of increased phosphorylation, we have strong reason to believe that Akt activity is effectively increased, although we will continue to investigate this further. Finally, fractionating cardiomyocytes into cytosolic and nuclear

components, we found a shift towards earlier phoshorylation of Akt at Ser473 in cells lacking PHLPP1. The goal to characterize PHLPP in AMVM is still in its beginning stages, but new insights into how PHLPP1 removal effects Akt will pave the way for future research prospects.

More research still needs to be done to characterize PHLPP in adult mouse ventricular myocytes. In addition to repeating experiments for tighter and more reliable data, the future direction in PHLPP research should determine if PHLPP removal has any physiological changes on the cardiomyocytes. Since Akt is involved in cell cycle regulation and proliferation, it would be interesting to see if removing PHLPP1 would result in any quantifiable differences in final cardiac myocyte number during development due to increased activation of Akt. Obtaining heart sections and counting cell number or counting nuclei per individual myocyte may provide answers on that front. Furthermore, Brognard et al have published data showing that there is PHLPP isoform specificity for different Akt isoforms and downstream targets in immortalized cell lines. This data became available only after we had generated *PHLPP1*$^{-/-}$ mice. Therefore, another facet of PHLPP research would be to determine if there is PHLPP specificity for Akt isoforms in cardiomyocytes. Data from knockdown studies done in neonatal rat ventricular myocytes suggest that this specificity does not exist in cardiomyocytes (Shigeki, data unpublished), however adult and neonatal myocytes are fundamentally different which makes it hard to extrapolate data from one to the other. Investigating isoform specificity in AMVM will be more applicable to adult humans suffering from cardiac hypertrophy and it may also provide an explanation for the differential downstream target phosphorylation seen earlier. Currently *PHLPP2*$^{-/-}$ mice are being

generated and eventually we will aim to generate double knockout mice. Possibly the most pertinent physiological question that needs to be addressed is what protective effects will PHLPP removal have on individual cardiomyocytes. Members in our lab are currently conducting *in vivo* studies comparing transverse aortic constriction (TAC) and exercise-induced cardiac hypertrophy and the protective potential by loss of PHLPP1. Similary, apoptosis assays performed on cultured cardiomyocytes could elucidate the extent of protection afforded to individual cells by increased Akt activity as a result in loss of PHLPP. Regardless of the direction in which PHLPP research progresses, in the context of the cardiac community it will all be for the unanimous effort to determine the regulatory properties of Akt signaling on the hearts hypertrophic response in an adaptive or maladaptive manner. Any additional data brings us that much closer to understanding the complex signal transduction mechanisms involved in disease progression, thus giving scientists and physicians the advantage to be able to develop specific and effective therapies and treatments against pathological cardiac hypertrophy.

Appendix

Tables of Buffers and Medias

Table 0.1 – 10mM $CaCl_2$, Volume: 25 ml

Reagent	Source	F.W. or Stock Conc.	Quantity	Final Conc.
Calcium Chloride Anhydrous ($CaCl_2$)	Fisher Scientific	111.0 g/mol	0.028 g	10 mM

Table 0.1a – 100mM $CaCl_2$, Volume: 25 ml

Reagent	Source	F.W. or Stock Conc.	Quantity	Final Conc.
$CaCl_2$	Fisher Scientific	111.0 g/mol	0.278 g	100 mM

1. Dissolve $CaCl_2$ in 15 ml Millipore water.
2. Bring volume up to 25 ml.
3. Filter-sterilize using Millipore Steriflip.
4. Store at room temperature.

Table 0.2 – 500mM 2-3, Butanedione monoxime (BDM), Volume: 50 ml

Reagent	Source	F.W. or Stock Conc.	Quantity	Final Conc.
2-3, Butanedione monoxime (BDM)	Sigma-Aldrich	101.1 g/mol	2.528 g	500 mM

1. Weigh out BDM under a covered balance – DO NOT BREATHE IN BDM.
2. Dissolve BDM in 25 ml Millipore water.
3. Bring up volume to 50 ml with Millipore water.
4. Filter-sterilize using Millipore Steriflip.
5. Store at -20˚C.

Table 0.3 – 6.25mg/ml Liberase Blendzyme 1, Volume: 14.4 ml

Reagent	Source	F.W. or Stock Conc.	Quantity	Final Conc.
Liberase Blendzyme 1	Roche Diagnostics	90 mg	1 bottle	6.25 mg/ml

1. Add 10 ml Millipore water to bottle containing 90 mg Liberase Blendzyme 1.
2. Put the original cap back on and invert several times. Make sure to dissolve any enzyme that may have been on the cap.
3. Vortex to ensure enzyme thoroughly dissolved.
4. Carefully remove cap and add 4.4 ml Millipore water.

5. Pipette up and down a couple times to mix well.
6. Make 1 ml aliquots of the Liberase Blendzyme 1.
7. Store at -20˚C.

Table 1.1 – 1X Stock Perfusion buffer, Volume: 1L

Reagent	Source	F.W. or Stock Conc.	Quantity	Final Conc.
Sodium Chloride (NaCl)	Fisher Scientific	58.4 g/mol	6.6 g	113 mM
Potassium Chloride (KCl)	Fisher Scientific	74.6 g/mol	0.35 g	4.7 mM
Potassium phosphate monobasic (KH_2PO_4)	Fisher Scientific	136.1 g/mol	0.082 g	0.6 mM
Sodium phosphate dibasic (Na_2HPO_4)	Fisher Scientific	142 g/mol	0.085 g	0.6 mM
Magnesium sulfate heptahydrate ($MgSO_4$-$7H_2O$)	Fisher Scientific	246.5 g/mol	0.3 g	1.2 mM
Sodium bicarbonate ($NaHCO_3$)	Fisher Scientific	84 g/mol	1.01 g	12mM
Potassium bicarbonate ($KHCO_3$)	Fisher Scientific	101 g/mol	1.01 g	10 mM
Taurine	Sigma-Aldrich	125.1 g/mol	3.75 g	30 mM
HEPES buffer solution, 1M	GIBCO/Invitrogen	1 M	10 ml	10 mM

1. Add all components to 500 ml Millipore water.
2. Stir until all components thoroughly dissolved and bring volume up to 1L in graduated cylinder.
3. Sterilize solution via filtration.
4. Store at 4˚C up to 1 week.

Table 1.1a – Perfusion buffer, pH 7.46, Volume: 500 ml

Reagent	Source	F.W. or Stock Conc.	Quantity	Final Conc.
1X Stock Perfusion Buffer	See Table 1.1	1X	~500 ml	0.98X

Table 1.1a (cont.)

Reagent	Source	F.W. or Stock Conc.	Quantity	Final Conc.
BDM	Sigma-Aldrich	101.1 g/mol	0.5 g	10 mM
Glucose	Sigma-Aldrich	180.2 g/mol	0.5 g	5.5 mM

1. Add all components to 400 ml 1X Stock Perfusion Buffer.
2. Stir until all components thoroughly dissolved and bring volume up to 500 ml in graduated cylinder.
3. Sterilize solution via filtration.
4. Store at 4˚C up to 24 hours.

Table 1.2 – Myocyte digestion buffer, Volume: 25 ml

Reagent	Source	F.W. or Stock Conc.	Quantity	Final Conc.
Perfusion buffer, pH 7.46	See Table 1.1a	1X	25 ml	1X
Liberase blendzyme 1	See Table 0.3	6.25 mg/ml	1 ml	0.25 mg/ml
Trypsin	GIBCO/Invitrogen	10X	139 µl	0.14 mg/ml
Calcium chloride ($CaCl_2$)	See Table 0.1a	100 mM	3.125 µl	12.5 µM

1. Add all components to 25 ml Perfusion buffer, pH 7.46.
2. Mix by inversion.
3. Sterilize via filtration.
4. Do not store solution; prepare fresh as needed.

Table 1.3 – Myocyte stopping buffer 1, Volume: 10 ml

Reagent	Source	F.W. or Stock Conc.	Quantity	Final Conc.
Perfusion buffer, pH 7.46	See Table 1.1a	1X	9 ml	1X
Bovine calf serum (BCS)	Omega Scientific	100%	1 ml	10%
$CaCl_2$	See Table 0.1a	100 mM	1.25 µl	12.5 µM

1. Add all components to 9 ml Perfusion buffer, pH 7.46.
2. Mix by inversion.
3. Sterilize via filtration.
4. Do not store solution; prepare fresh as needed.

Table 1.4 – Myocyte stopping buffer 2, Volume: 30 ml

Reagent	Source	F.W. or Stock Conc.	Quantity	Final Conc.
Perfusion buffer, pH 7.46	See Table 1.1a	1X	28.5 ml	1X
BCS	Omega Scientific	100%	1.5 ml	5%
$CaCl_2$	See Table 0.1a	100 mM	3.75 µl	12.5 µM

1. Add all components to 28.5 ml Perfusion buffer, pH 7.46.
2. Mix by inversion.
3. Sterilize via filtration.
4. Do not store solution; prepare fresh as needed.

Table 2.1 – Myocyte plating medium, Volume: 49.5 ml

Reagent	Source	F.W. or Stock Conc.	Quantity	Final Conc.
Minimum essential medium (MEM), 1X (with Hanks' salts and L-glutamine	GIBCO/Invitrogen	1X	45 ml	0.9X
BCS	Omega Scientific	100%	2.5 ml	5%
2,3-Butanedione monoxime (BDM)	See Table 0.2	500 mM	1 ml	10 mM
Penicillin	GIBCO/Invitrogen	10,000 U/ml	0.5 ml	100 U/ml
L-Glutamine	GIBCO/Invitrogen	200 mM	0.5 ml	2 mM

1. Sterilely add all components to 45 ml MEM.
2. Sterilize via filtration.
3. Equilibrate medium overnight in a 2% CO_2 incubator at 37˚C to adjust temperature and pH balance of the medium. Final pH should be approximately 7.
4. Store at 37˚C in 2% CO_2 incubator up to 1 week.

Table 2.2 – Myocyte culture medium, Volume: 46.5 ml

Reagent	Source	F.W. or Stock Conc.	Quantity	Final Conc.
Minimum essential medium (MEM), 1X (with Hanks' salts and L-glutamine	GIBCO/Invitrogen	1X	45 ml	0.9X

Table 2.2 (cont.)

Reagent	Source	F.W. or Stock Conc.	Quantity	Final Conc.
Myocyte bovine serum albumin (MC BSA)	EMD Chemicals	100 mg/ml	50 µl	0.1 mg/ml
Penicillin	GIBCO/Invitrogen	10,000 U/ml	0.5 ml	100 U/ml
L-Glutamine	GIBCO/Invitrogen	200 mM	0.5 ml	2 mM

1. Sterilely add all components to 45 ml MEM.
2. Sterilize via filtration.
3. Equilibrate medium overnight in a 2% CO_2 incubator at 37˚C to adjust temperature and pH balance of the medium. Final pH should be approximately 7.
4. Store at 37˚C in 2% CO_2 incubator up to 1 week.

Table 2.2a – Myocyte culture medium with BDM, Volume: as needed

Reagent	Source	F.W. or Stock Conc.	Quantity	Final Conc.
Myocyte culture medium	See Table 2.2	1X	As needed (ml)	1X
2,3-Butanedione monoxime (BDM)	See Table 0.2	500 mM	As needed (µl)	10 mM

1. Calculate amount Myocyte culture medium needed.
2. Calculate amount BDM needed using (500mM)(V)=(10mM)(MC culture)
3. Add required amount of 500 mM BDM to needed amount of Myocyte culture medium.
4. Sterilize via filtration.
5. Replace Myocyte plating medium on isolated adult mouse ventricular myocytes (AMVMs) with Myocyte culture medium with BDM and leave overnight.

Table 3.1 – Laminin coating solution; Volume: 6 ml

Reagent	Source	F.W. or Stock Conc.	Quantity	Final Conc.
Laminin stock solution	Invitrogen	1 mg/ml	60 µl	10 µg/ml
Dulbecco's Phosphate buffered saline (PBS), 1X ($CaCl_2$/$MgCl_2$-free)	GIBCO/Invitrogen	1X	6 ml	1X

1. Calculate how much laminin coating solution is needed. Every one 60 µl-aliquot of laminin stock solution makes 6 ml of laminin.
2. Mix by inversion.
3. Distribute enough laminin to cover the bottom of dishes and wells.
4. Allow laminin to coat dishes and wells overnight at 37˚C in a 2% CO_2 incubator.
5. Store at 37˚C in the 2% CO_2 incubator until needed. Discard dish or plate if laminin coating solution has evaporated.

Table 4.1 – Leukemia inhibitory factor (LIF), Volume: 100 µl

Reagent	Source	F.W. or Stock Conc.	Quantity	Final Conc.
ESGRO (LIF)	Chemicon International	$1x10^7$ units/ml	10 µl	5 µM
PBS	GIBCO/Invitrogen	1X	90 µl	1X

1. In a clean microfuge tube add 90 µl PBS.
2. Add 10 µl LIF and pipette up and down to mix.
3. Store at 4˚C.

Table 5.1 – 5X SDS loading buffer, Volume: 48 ml

Reagent	Source	F.W. or Stock Conc.	Quantity	Final Conc.
1M Tris	Self-made stock	1 M	12 ml	250 mM
Glycerol	Fisher Scientific	100%	19.2 ml	40%
Sodium dodecyl sulfate (SDS)	EMD	288.4 g/mol	3.84 g	277 mM
β-mercaptoethanol	Sigma Aldrich	14.2 M	9.6 ml	$2.84x10^3$ mM
Bromophenol blue	Fisher Scientific	670.0 g/mol	0.048 g	1.5 mM

1. Combine components and stir well.
2. Aliquot appropriately.
3. Store at -20˚C.

Table 6.1 – NuPage Running buffer for Western blotting, Volume: 4 L

Reagent	Source	F.W. or Stock Conc.	Quantity	Final Conc.
NuPage (MOPS or TA) Running Buffer	Invitrogen	20X	200 ml	1X
NuPage Antioxidant	Invitrogen	100%	10 ml	0.25%

1. Combine NuPage running buffer and antioxidant.

2. Bring volume up to 4 L with Millipore water.
3. Store at room 4˚C.

Table 6.2 – 1X NuPage Transfer buffer, Volume: 1 L

Reagent	Source	F.W. or Stock Conc.	Quantity	Final Conc.
NuPage Transfer Buffer	Invitrogen	20X	50 ml	1X
Methanol	Fisher Scientific	100%	200 ml	20%

1. Combine NuPage Transfer buffer and Methanol in 1 L graduated cylinder.
2. Bring volume up to 1 L with Millipore water.
3. Store at 4˚C.

Table 6.3 – 10X Tris-Buffered saline (TBS), Volume: 4 L

Reagent	Source	F.W. or Stock Conc.	Quantity	Final Conc.
Tris-HCl	EMD Chemicals	157.6 g/mol	63 g	100 mM
NaCl	Fisher Scientific	58.4 g/mol	70.2 g	300 mM

1. Dissolve components in 2 L Millipore water.
2. Bring up to 4 L with Millipore water and pH to 7.5.
3. Store at room temperature.

Table 6.3a – 1X TBS with 0.1% Tween, Volume: 20 L

Reagent	Source	F.W. or Stock Conc.	Quantity	Final Conc.
Tris-Buffered Saline (TBS)	Table 6.3	10X	2000 ml	1X
Tween-20	Fisher Scientific	100%	20 ml	0.1%

1. Combine TBS and Tween-20.
2. Bring up to 20 L with Millipore water.
3. Store at room temperature.

Table 6.4 – 5% milk/TBS-T, Volume: 100 ml

Reagent	Source	F.W. or Stock Conc.	Quantity	Final Conc.
Powdered milk	Safeway	NA	5 g	5%
TBS-T	Table 6.3	1X	100 ml	1X

1. Weigh out 5 g powdered milk and dissolve in 50 ml TBS-T.
2. Bring volume to 100 ml with TBS-T.
3. Keep on stir plate with stir bar.

4. Throw out at the end of the day.

Table 6.5 – 5% BSA/TBS-T, Volume: 50 ml

Reagent	Source	F.W. or Stock Conc.	Quantity	Final Conc.
Bovine Serum Albumin (BSA), Fraction V	EMD Chemicals	N/A	2.5 g	5%
TBS-T	Table 6.3	1X	50 ml	1X
Sodium Azide (NaN_3)	Sigma Aldrich	10%	100µl	0.02%

1. Weigh out 2.5 g BSA and dissolve in 25 ml TBS-T.
2. Bring volume to 50 ml with TBS-T.
3. Keep on stir plate with stir bar.
4. Add NaN_3 and mix by inverting several times.
5. Store at 4˚C.

Table 7.1 – Western Buffer, Volume: 500 ml

Reagent	Source	F.W. or Stock Conc.	Quantity	Final Conc.
Sodium Phosphate	Self-made Stock	0.5 M	20 ml	20 mM, pH 7
Sodium Chloride	Self-made Stock	5 M	15 ml	150 mM
Magnesium Chloride	Self-made Stock	1 M	1 ml	2 mM
NP-40	Sigma Aldrich	100%	0.5 ml	0.1%
Glycerol	Fisher Scientific	100%	50 ml	10%
Okadaic acid	Sigma Aldrich	10 µM	0.5 ml	10 nM
Sodium Fluoride	Sigma Aldrich	1 M	5 ml	10 mM
Sodium Pyrophosphate	Sigma Aldrich	0.5 M	10 ml	10 mM
DTT	Sigma Aldrich	1 M	0.5 ml	1 mM
Na_3VO_4	Sigma Aldrich	200mM	0.0092 g	0.1 mM
Pepstatin	Sigma Aldrich	1 mg/ml	5 ml	10 µg/ml
Leupeptin	Sigma Aldrich	1 mg/ml	5 ml	10 µg/ml
Aprotinin	Sigma Aldrich	25 mg/ml	200 µl	10 µg/ml
TLCK	Sigma Aldrich	5 mg/ml	1 ml	10 µg/ml
TPCK	Sigma Aldrich	5 mg/ml	1 ml	10 µg/ml

1. Add components to 250 ml Millipore water.
2. Bring volume up to 500 ml and mix well.

3. Aliquot as needed and store at -20˚C.

Table 8.1 – Buffer C, Volume: 100 ml

Reagent	Source	F.W. or Stock Conc.	Quantity	Final Conc.
Hepes pH7.6	Fisher Scientific	238.3 g/mol	0.2383 g	10 mM
NaCl	Fisher Scientific	58.4 g/mol	0.0584 g	10 mM
$MgCl_2 \cdot 6H_2O$	Fisher Scientific	203.3 g/mol	0.0305 g	1.5 mM
Glycerol	Fisher Scientific	100%	10 ml	10%

1. Dissolve Hepes in about 50 ml Millipore water and pH to 7.6.
2. Dissolve NaCl and $MgCl_2$ in the Hepes pH 7.6 solution.
3. Add glycerol.
4. Bring final volume to 100 ml with Millipore water.

Table 8.2 – High Salt RIPA buffer, Volume: 100 ml

Reagent	Source	F.W. or Stock Conc.	Quantity	Final Conc.
Tris-HCl pH 7.4	Self-made Stock	1 M	5 ml	50 mM
NaCl	Fisher Scientific	58.4 g/mol	2.92 g	500 mM
EDTA	Sigma Aldrich			1 mM
Triton-X	Sigma Aldrich	100%	1 ml	1%
Na deoxycholate	Sigma Aldrich	414.6 g/mol	0.1 g	1%
SDS	EMD	288.4 g/mol	0.1 g	0.1%

Table 8.3 – Buffers with protease inhibitors cocktail, Volume: 1 ml

Reagent	Source	F.W. or Stock Conc.	Quantity	Final Conc.
PBS/C/RIPA Buffer	GIBCO/Invitrogen Table 8.1 or Table 8.2	1X	1 ml	1X
PNPP	Sigma Aldrich	1 M	1 µl	1 mM
Leupeptin	Sigma Aldrich	10µg/µl	1 µl	10 µg
Aprotinin	Sigma Aldrich	200X	5 µl	1X
PMSF	Sigma Aldrich	100mM	10 µl	1 mM

Table 9.1 – 4% Paraformaldehyde (PFA), Volume: 500 ml

Reagent	Source	F.W. or Stock Conc.	Quantity	Final Conc.
Para-formaldehyde	Sigma Aldrich	(30.03)n g/mol	20 g	4%
PBS	GIBCO/Invitrogen	1X	~500 ml	1X
Sodium Hydroxide (NaOH)	EM Science	40.0 g/mol	As needed	As needed

1. Add the paraformaldehyde to 400 ml PBS in a glass beaker.
2. Heat with stirring to about 60˚C (solution should become clear).
3. Add 0.1 M NaOH drop wise until pH ~7.
4. Bring up volume to 500 ml with PBS.
5. Filter-sterilize and store at room temperature.

Table 9.2 – 0.2% Triton-X, Volume: 300 ml

Reagent	Source	F.W. or Stock Conc.	Quantity	Final Conc.
Triton-X	Sigma Aldrich	100%	600 µl	0.2%
PBS	GIBCO/Invitrogen	1X	300 ml	1X

1. Cut 1 ml pipette tip with barrier.
2. Slowly pipette the needed amount of Triton-X (viscous).
3. Pipette into PBS and keep pipetting up and down until as much Triton-X dissolved as possible.
4. Mix until all Triton-X dissolved.
5. Store at room temperature.

Table 9.3 – Immunocytochemistry (IC) Block, Volume: 250 ml

Reagent	Source	F.W. or Stock Conc.	Quantity	Final Conc.
BSA, Fraction V	EMD Chemicals	N/A	5 g	2%
Goat Serum	Sigma Aldrich	100%	25 ml	10%
Triton-X	Sigma Aldrich	100%	250 µl	0.1%
PBS	GIBCO/Invitrogen	1X	250 ml	1X

1. Add all components to 100 ml PBS and stir well.
2. Bring final volume up to 250 ml. Aliquot appropriately.
3. Store at -20˚C

Table 10.1 – 6X Kinase Buffer, Volume: 5 ml

Reagent	Source	F.W. or Stock Conc.	Quantity	Final Conc.
Hepes, pH 7.6	Self-made Stock	1 M	600 µl	120 mM
$MgCl_2$	Self-made Stock	1 M	600 µl	120 mM
DTT	Sigma Aldrich	1 M	60 µl	12 mM
β-Glycerophosphate	Sigma Aldrich	0.5 M	1.2 ml	120 mM
PNPP	Simga Aldrich	1 M	600 µl	120 mM
Na_3VO_4	Sigma Aldrich	500 mM	3 µl	300 µM

1. Add components to 1 ml of water.
2. Bring final volume to 5 ml and invert to mix. Aliquot appropriately.
3. Store at -20˚C.

Table 10.2 – Kinase Reaction Mixture, Volume: 30 µl

Reagent	Source	F.W. or Stock Conc.	Quantity	Final Conc.
Kinase Buffer	Table 10.1	6X	5 µl	1X
GSK3 Fusion Protein	Cell Signaling Technology (9237)	1 mg/ml	1 µl	1 µg
ATP	Self-made Stock	5 mM	1.2 µl	200 µM
Water	N/A	1X	22.8 µl	1X

Table of Antibodies

Table 1.1 – Primary Antibody

Antibody	MW (kDa)	Host	Store (˚C)	Dilution	Manufacturer	Catalog No.
GAPDH	36	Rabbit	-20	1:1000	Cell Signaling	2118
α-Tubulin	46	Mouse	4	1:1000	Santa Cruz	Sc-8035
Lamin A/C	70	Rabbit	-20	1:1000	Cell Signaling	2032
RhoGDI	28	Mouse	-20	1:1000	BD Biosciences	61025S
pAktSer473	60	Rabbit	-20	1:1000	Cell Signaling	9271
pAktThr308	60	Rabbit	-20	1:1000	Cell Signaling	9275
Total-Akt	60	Rabbit	-20	1:1000	Cell Signaling	9272
PHLPP1β	180	Rabbit	4	1:2000	Bethyl	A300-660A-1
PHLPP2	150	Rabbit	4	1:2000	Bethyl	A300-661A
pMDM2	90	Rabbit	-20	1:1000	Cell Signaling	3521
pGSK3α/β	51/46	Rabbit	-20	1:1000	Cell Signaling	9331S
pERK1/2	42/44	Rabbit	-20	1:1000	Cell Signaling	9101

1. Dilute primary antibody in 5% BSA/TBS-T with 0.02% NaN_3 (Buffers and Media List Table 6.5).
2. Store at 4˚C.

Table 1.2 – Secondary Antibody

Antibody	Conjugated to	Store (˚C)	Dilution	Manufacturer	Catalog No.
Anti-Rabbit IgG	Horse Radish Peroxidase	4	1:2000	Sigma Aldrich	A0545
Anti-Mouse IgG	Horse Radish Peroxidase	4	1:2000	Sigma Aldrich	A5278

1. Dilute secondary antibody in 5% milk/TBS-T (Buffers and Media List Table 6.4).
2. One time usage. Make fresh as needed.

Table 2.1 – Immunofluorescence Antibody

Antibody	Conjugated to	Store (˚C)	Final Dilution	Manufacturer	Catalog No.
α-actinin	Mouse	-20	1:500	Sigma Aldrich	A7811
Lectin from Triticum vulgaris (WGA)	FITC	-20	1:200	Sigma Aldrich	L4895
Anti-Mouse Alexa594	TRITC	-20	1:4000	Invitrogen	A21044

1. Dilute antibody in IC Block (Buffers and Media List Table 9.3) and keep covered from light.
2. One time usage. Make fresh as needed.

Table 2.2 – Mounting Media

Media	Type	Store (˚C)	Manufacturer	Catalog No.
Vectashield	Hard Set with DAPI	4	Vector Laboratories	H-1500

1. Add one drop to each chamber (two drops total).
2. Carefully place coverslip over slide and push all bubbles to the side.
3. Let Vectashield dry overnight at room temperature.
4. Store stock Vectashield at 4˚C.

Table 3.1 – Immunoprecipitation Antibody

Antibody	MW (kDa)	Host	Store (˚C)	Dilution	Manufacturer	Catalog No.
Total-Akt	60	Mouse	-20	1:100	Cell Signaling	2966

1. Add antibody directly into immunoprecipitation setup.

References

1. (2009) FastStats - Heart Disease.

2. Heineke, J., and Molkentin, J.D. (2006) Regulation of cardiac hypertrophy by intracellular signalling pathways. Nat Rev Mol Cell Biol 7, 589-600.

3. Lloyd-Jones, D., Adams, R., Carnethon, M., De Simone, G., Ferguson, T.B., Flegal, K., Ford, E., Furie, K., Go, A., Greenlund, K., Haase, N., Hailpern, S., Ho, M., Howard, V., Kissela, B., Kittner, S., Lackland, D., Lisabeth, L., Marelli, A., McDermott, M., Meigs, J., Mozaffarian, D., Nichol, G., O'Donnell, C., Roger, V., Rosamond, W., Sacco, R., Sorlie, P., Stafford, R., Steinberger, J., Thom, T., Wasserthiel-Smoller, S., Wong, N., Wylie-Rosett, J., and Hong, Y. (2009) Heart disease and stroke statistics--2009 update: a report from the American Heart Association Statistics Committee and Stroke Statistics Subcommittee. Circulation 119, 480-486.

4. Frey, N., and Olson, E.N. (2003) Cardiac hypertrophy: the good, the bad, and the ugly. Annu Rev Physiol 65, 45-79.

5. Walsh, K. (2006) Akt signaling and growth of the heart. Circulation 113, 2032-2034.

6. Ghofrani, H.A., Barst, R.J., Benza, R.L., Champion, H.C., Fagan, K.A., Grimminger, F., Humbert, M., Simonneau, G., Stewart, D.J., Ventura, C., and Rubin, L.J. (2009) Future perspectives for the treatment of pulmonary arterial hypertension. J Am Coll Cardiol 54, S108-117.

7. Catalucci, D., Latronico, M.V., Ellingsen, O., and Condorelli, G. (2008) Physiological myocardial hypertrophy: how and why? Front Biosci 13, 312-324.

8. Mahdavi, V., Chambers, A.P., and Nadal-Ginard, B. (1984) Cardiac alpha- and beta-myosin heavy chain genes are organized in tandem. Proc Natl Acad Sci U S A 81, 2626-2630.

9. Konhilas, J.P., and Leinwand, L.A. (2006) Partnering up for cardiac hypertrophy. Circ Res 98, 985-987.

10. Klaassen, L.J.C.J.D.C.D. (2001) Casarett and Doull's Toxicology: The Basic Science of Poisons. New York: McGraw-Hill Medical Pub. Division.

11. Neyses, L., and Pelzer, T. (1995) The biological cascade leading to cardiac hypertrophy. Eur Heart J 16 Suppl N, 8-11.

12. Gao, D., Inuzuka, H., Tseng, A., and Wei, W. (2009) Akt finds its new path to regulate cell cycle through modulating Skp2 activity and its destruction by APC/Cdh1. Cell Div 4, 11.

13. Calleja, V., Laguerre, M., and Larijani, B. (2009) 3-D structure and dynamics of protein kinase B-new mechanism for the allosteric regulation of an AGC kinase. J Chem Biol 2, 11-25.

14. Sale, E.M., and Sale, G.J. (2008) Protein kinase B: signalling roles and therapeutic targeting. Cell Mol Life Sci 65, 113-127.

15. Laine, J., Kunstle, G., Obata, T., and Noguchi, M. (2002) Differential regulation of Akt kinase isoforms by the members of the TCL1 oncogene family. J Biol Chem 277, 3743-3751.

16. Zinda, M.J., Johnson, M.A., Paul, J.D., Horn, C., Konicek, B.W., Lu, Z.H., Sandusky, G., Thomas, J.E., Neubauer, B.L., Lai, M.T., and Graff, J.R. (2001) AKT-1, -2, and -3 are expressed in both normal and tumor tissues of the lung, breast, prostate, and colon. Clin Cancer Res 7, 2475-2479.

17. Matheny, R.W., Jr., and Adamo, M.L. (2009) Current perspectives on Akt Akt-ivation and Akt-ions. Exp Biol Med (Maywood).

18. Shiojima, I., and Walsh, K. (2006) Regulation of cardiac growth and coronary angiogenesis by the Akt/PKB signaling pathway. Genes Dev 20, 3347-3365.

19. Mendoza, M.C., and Blenis, J. (2007) PHLPPing it off: phosphatases get in the Akt. Mol Cell 25, 798-800.

20. DeBosch, B., Sambandam, N., Weinheimer, C., Courtois, M., and Muslin, A.J. (2006) Akt2 regulates cardiac metabolism and cardiomyocyte survival. J Biol Chem 281, 32841-32851.

21. Miyamoto, S., Rubio, M., and Sussman, M.A. (2009) Nuclear and mitochondrial signalling Akts in cardiomyocytes. Cardiovasc Res 82, 272-285.

22. DeBosch, B., Treskov, I., Lupu, T.S., Weinheimer, C., Kovacs, A., Courtois, M., and Muslin, A.J. (2006) Akt1 is required for physiological cardiac growth. Circulation 113, 2097-2104.

23. Clerk, A., Cullingford, T.E., Fuller, S.J., Giraldo, A., Markou, T., Pikkarainen, S., and Sugden, P.H. (2007) Signaling pathways mediating cardiac myocyte gene expression in physiological and stress responses. J Cell Physiol 212, 311-322.

24. Ben-Shlomo, A., Miklovsky, I., Ren, S.G., Yong, W.H., Heaney, A.P., Culler, M.D., and Melmed, S. (2003) Leukemia inhibitory factor regulates prolactin secretion in prolactinoma and lactotroph cells. J Clin Endocrinol Metab 88, 858-863.

25. Falconi, D., Oizumi, K., and Aubin, J.E. (2007) Leukemia inhibitory factor influences the fate choice of mesenchymal progenitor cells. Stem Cells 25, 305-312.

26. Howes, A.L., Arthur, J.F., Zhang, T., Miyamoto, S., Adams, J.W., Dorn, G.W., 2nd, Woodcock, E.A., and Brown, J.H. (2003) Akt-mediated cardiomyocyte survival pathways are compromised by G alpha q-induced phosphoinositide 4,5-bisphosphate depletion. J Biol Chem 278, 40343-40351.

27. King, K.L., Winer, J., Phillips, D.M., Quach, J., Williams, P.M., and Mather, J.P. (1998) Phenylephrine, endothelin, prostaglandin F2alpha' and leukemia inhibitory factor induce different cardiac hypertrophy phenotypes in vitro. Endocrine 9, 45-55.

28. Gao, T., Furnari, F., and Newton, A.C. (2005) PHLPP: a phosphatase that directly dephosphorylates Akt, promotes apoptosis, and suppresses tumor growth. Mol Cell 18, 13-24.

29. Miyamoto, S., Murphy, A.N., and Brown, J.H. (2008) Akt mediates mitochondrial protection in cardiomyocytes through phosphorylation of mitochondrial hexokinase-II. Cell Death Differ 15, 521-529.

30. Manning, B.D., and Cantley, L.C. (2007) AKT/PKB signaling: navigating downstream. Cell 129, 1261-1274.

31. Latronico, M.V., Costinean, S., Lavitrano, M.L., Peschle, C., and Condorelli, G. (2004) Regulation of cell size and contractile function by AKT in cardiomyocytes. Ann N Y Acad Sci 1015, 250-260.

32. Yang, Z.Z., Tschopp, O., Baudry, A., Dummler, B., Hynx, D., and Hemmings, B.A. (2004) Physiological functions of protein kinase B/Akt. Biochem Soc Trans 32, 350-354.

33. Schiekofer, S., Shiojima, I., Sato, K., Galasso, G., Oshima, Y., and Walsh, K. (2006) Microarray analysis of Akt1 activation in transgenic mouse hearts reveals transcript expression profiles associated with compensatory hypertrophy and failure. Physiol Genomics 27, 156-170.

34. Yang, Z.Z., Tschopp, O., Di-Poi, N., Bruder, E., Baudry, A., Dummler, B., Wahli, W., and Hemmings, B.A. (2005) Dosage-dependent effects of Akt1/protein kinase Balpha (PKBalpha) and Akt3/PKBgamma on thymus, skin, and cardiovascular and nervous system development in mice. Mol Cell Biol 25, 10407-10418.

35. Sussman, M. (2007) "AKT"ing lessons for stem cells: regulation of cardiac myocyte and progenitor cell proliferation. Trends Cardiovasc Med 17, 235-240.

36. Calleja, V., Alcor, D., Laguerre, M., Park, J., Vojnovic, B., Hemmings, B.A., Downward, J., Parker, P.J., and Larijani, B. (2007) Intramolecular and intermolecular interactions of protein kinase B define its activation in vivo. PLoS Biol 5, e95.

37. Shimizu, K., Okada, M., Takano, A., and Nagai, K. (1999) SCOP, a novel gene product expressed in a circadian manner in rat suprachiasmatic nucleus. FEBS Lett 458, 363-369.

38. Brognard, J., and Newton, A.C. (2008) PHLiPPing the switch on Akt and protein kinase C signaling. Trends Endocrinol Metab 19, 223-230.

39. Brognard, J., Sierecki, E., Gao, T., and Newton, A.C. (2007) PHLPP and a second isoform, PHLPP2, differentially attenuate the amplitude of Akt signaling by regulating distinct Akt isoforms. Mol Cell 25, 917-931.

40. Liao, R., and Jain, M. (2007) Isolation, culture, and functional analysis of adult mouse cardiomyocytes. Methods Mol Med 139, 251-262.

41. McCurdy, S., Baicu, C.F., Heymans, S., and Bradshaw, A.D. (2009) Cardiac extracellular matrix remodeling: Fibrillar collagens and Secreted Protein Acidic and Rich in Cysteine (SPARC). J Mol Cell Cardiol.

42. Mitcheson, J.S., Hancox, J.C., and Levi, A.J. (1998) Cultured adult cardiac myocytes: future applications, culture methods, morphological and electrophysiological properties. Cardiovasc Res 39, 280-300.

43. Chlopcikova, S., Psotova, J., and Miketova, P. (2001) Neonatal rat cardiomyocytes--a model for the study of morphological, biochemical and electrophysiological characteristics of the heart. Biomed Pap Med Fac Univ Palacky Olomouc Czech Repub 145, 49-55.

44. Korhonen, T., Hanninen, S.L., and Tavi, P. (2009) Model of excitation-contraction coupling of rat neonatal ventricular myocytes. Biophys J 96, 1189-1209.

45. Sadoshima, J., and Izumo, S. (1997) The cellular and molecular response of cardiac myocytes to mechanical stress. Annu Rev Physiol 59, 551-571.

46. Rota, M., Hosoda, T., De Angelis, A., Arcarese, M.L., Esposito, G., Rizzi, R., Tillmanns, J., Tugal, D., Musso, E., Rimoldi, O., Bearzi, C., Urbanek, K., Anversa, P., Leri, A., and Kajstura, J. (2007) The young mouse heart is composed of myocytes heterogeneous in age and function. Circ Res 101, 387-399.

47. O'Connell, T.D., Rodrigo, M.C., and Simpson, P.C. (2007) Isolation and culture of adult mouse cardiac myocytes. Methods Mol Biol 357, 271-296.

48. Li, X., Zima, A.V., Sheikh, F., Blatter, L.A., and Chen, J. (2005) Endothelin-1-induced arrhythmogenic Ca2+ signaling is abolished in atrial myocytes of inositol-1,4,5-trisphosphate(IP3)-receptor type 2-deficient mice. Circ Res 96, 1274-1281.

49. Maillet, M., Purcell, N.H., Sargent, M.A., York, A.J., Bueno, O.F., and Molkentin, J.D. (2008) DUSP6 (MKP3) null mice show enhanced ERK1/2 phosphorylation at baseline and increased myocyte proliferation in the heart affecting disease susceptibility. J Biol Chem 283, 31246-31255.

50. De Windt, L.J., Lim, H.W., Haq, S., Force, T., and Molkentin, J.D. (2000) Calcineurin promotes protein kinase C and c-Jun NH2-terminal kinase activation in the heart. Cross-talk between cardiac hypertrophic signaling pathways. J Biol Chem 275, 13571-13579.

51. Ryan, K.E., Casey, S.M., Canty, M.J., Crowe, M.A., Martin, F., and Evans, A.C. (2007) Akt and Erk signal transduction pathways are early markers of differentiation in dominant and subordinate ovarian follicles in cattle. Reproduction 133, 617-626.

52. Ryan, K.E., Glister, C., Lonergan, P., Martin, F., Knight, P.G., and Evans, A.C. (2008) Functional significance of the signal transduction pathways Akt and Erk in ovarian follicles: in vitro and in vivo studies in cattle and sheep. J Ovarian Res 1, 2.

53. Saxena, N.K., Sharma, D., Ding, X., Lin, S., Marra, F., Merlin, D., and Anania, F.A. (2007) Concomitant activation of the JAK/STAT, PI3K/AKT, and ERK signaling is involved in leptin-mediated promotion of invasion and migration of hepatocellular carcinoma cells. Cancer Res 67, 2497-2507.

54. Kruse, J.P., and Gu, W. (2009) Modes of p53 regulation. Cell 137, 609-622.

55. Rayasam, G.V., Tulasi, V.K., Sodhi, R., Davis, J.A., and Ray, A. (2009) Glycogen synthase kinase 3: more than a namesake. Br J Pharmacol 156, 885-898.